Dynamic Air Exchange Prosthesis: Effects on Heat Transfer and Limb Adherence for Active Lower Limb Amputees

Jonathan M. Schreven

A thesis

submitted in partial fulfillment of the

requirements for the degree of

Master of Science in Mechanical Engineering

University of Washington

2015

Committee:

Glenn K. Klute

Kat Steele

Dayong Gao

Program Authorized to Offer Degree:

Mechanical Engineering

University of Washington

Abstract

Dynamic Air Exchange Prosthesis: Effects on Heat
Transfer and Limb Adherence for Active Lower Limb Amputees

Jonathan M. Schreven

Chair of the Supervisory Committee:
Glenn K. Klute, Ph.D.
Mechanical Engineering

Lower limb amputees are often dissatisfied with the comfort of their prosthesis. A literature review of 38 selected studies revealed that more than 53% of people with amputation experienced heat and/or perspiration discomfort inside their prostheses. Current prosthetic liners are usually made from silicon, polyurethane or a combination polymer with a fabric outer layer and have thermally insulating properties. Lack of liner breathability and permeability also causes disproportionate amounts of moisture to pool against the skin. A novel new Dynamic Air Exchange (DAE) socket, being evaluated for this study, uses a small vacuum pump and pressure sensor to dynamically maintain a slight vacuum suction in the socket. Air is drawn in through four proximal liner ports, flows distally through a thin sock between the skin and liner, and forces perspiration and water vapor out a port in the prosthesis' distal locking pin. Analysis includes a computational model to show how heat removal varies in different thermal

environments, physical test results from a thermal manikin, and preliminary outcomes from human subject study results (n=2) comparing adherence between the DAE socket and a standard of care (SoC) pin lock socket. The DAE system removes moisture from the socket effectively but has little effect on overall skin temperature. The computational model suggests that cooling rates for current DAE socket airflow are near 3W for 20 °C ambient air and 10% relative humidity. Cooling rates increase to 29W when the flow velocity is increases from 0.03m/s (current DAE) to 0.5m/s under the same external conditions. Effects of varying flow velocity, relative humidity, and inlet air temperature on heat transfer rate are also presented.

DYNAMIC AIR EXCHANGE PROSTHESIS: EFFECTS ON HEAT TRANSFER AND LIMB ADHERENCE FOR ACTIVE LOWER LIMB AMPUTEES

[1]University of Washington, Department of Mechanical Engineering, Seattle, WA, USA

[2]Department of Veterans Affairs (VA), Rehabilitation Research and Development Center for Limb Loss Prevention and Prosthetic Engineering, VA Puget Sound, Seattle, WA, USA

LIST OF VARIABLES

r_i – $Radius\ of\ limb\ equivalent\ cylinder\ (m)$

r_o – $Outer\ radius\ of\ the\ sock\ layer\ (m)$

L – $Length\ of\ limb\ equivalent\ cylinder\ (m)$

A_s – $Surface\ area\ of the\ limb\ (m^2)$

A_{cs} – $Cross-sectional\ area\ of\ sock\ layer\ (m^2)$

$\dot{V}$ – $Volumetric\ flow\ rate\ of\ air\ through\ Dynamic\ Air\ Exchange\ socket\ \left(\frac{m^3}{s}\right)$

v – $Velocity\ of\ airflow\ through\ Dynamic\ Air\ Exchange\ socket\ \left(\frac{m}{s}\right)$

$\dot{m}_a$ – $Mass\ flow\ rate\ of\ dry\ air\ \left(\frac{kg}{s}\right)$

ρ_a – $Density\ of\ dry\ air\ \left(\frac{kg}{m^3}\right)$

R – $Specific\ gas\ constant\ of\ air\ \left(\frac{J}{kg\cdot K}\right)$

T_1 – $Entering\ air\ temperature\ (K)$

T_2 – $Exiting\ air\ temperature\ (K)$

T_{avg} – $Average\ air\ temperature\ inside\ Dynamic\ Air\ Exchange\ socket\ (K)$

T_{core} – *Body core temperature* (K)

$\dot{E}_{in}$ – *Internal energy flow of entering airflow* (W)

$\dot{W}_{in}$ – *Work energy flow for the control volume* (W)

$\dot{Q}_{in}$ – *Heat energy flow from the limb to the control volume* (W)

$\dot{E}_{out}$ – *Internal energy flow of exiting airflow* (W)

$\dot{m}_{a_1}$ – *Mass flow rate of entering dry air* $\left(\frac{kg}{s}\right)$

$\dot{m}_{a_2}$ – *Mass flow rate of exiting dry air* $\left(\frac{kg}{s}\right)$

$\dot{m}_{w_1}$ – *Mass flow rate of entering water vapor* $\left(\frac{kg}{s}\right)$

$\dot{m}_f$ – *Mass flow rate of perspiration* $\left(\frac{kg}{s}\right)$

$\dot{m}_{w_2}$ – *Mass flow rate of exiting water vapor* $\left(\frac{kg}{s}\right)$

ω_1 – *Specific humidity of entering air* $\left(\frac{kg\ H_2O}{kg\ dry\ air}\right)$

ω_2 – *Specific humidity of exiting air* $\left(\frac{kg\ H_2O}{kg\ dry\ air}\right)$

P_{atm} – *Atmospheric pressure at sea level* (Pa)

P_v – *Vapor pressure of water* (Pa)

P_g – *Saturated vapor pressure of water* (Pa)

φ – *Relative humidity* $\left(\frac{kg\ H_2O}{kg\ H_2O\ at\ saturation}\right)$

h_1 – *Enthalpy of entering humid air* $\left(\frac{kJ}{kg}\right)$

h_2 – *Enthalpy of exiting humid air* $\left(\frac{kJ}{kg}\right)$

h_{f_2} – *Enthalpy of exiting water vapor* $\left(\frac{kJ}{kg}\right)$

h_{g_1} – *Enthalpy of water vapor at* T_1 $\left(\frac{kJ}{kg}\right)$

h_{fg_2} – *Enthalpy of vaporization for water* $\left(\frac{kJ}{kg}\right)$

c_p – *Specific heat of dry air at constant pressure* $\left(\frac{kJ}{kg \cdot K}\right)$

R_{tissue} – *Equivalent thermal resistance of adipose tissue and skin tissue* $\left(\frac{K}{W}\right)$

R_{eq} – *Equivalent thermal resistance of* R_{tissue} *and surrounding air* $\left(\frac{K}{W}\right)$

h_c – *Convective heat transfer coefficient* $\left(\frac{W}{m^2 \cdot K}\right)$

t_{fat} – *Assumed thickness of adipose tissue* (m)

t_{skin} – *Assumed thickness of skin tissue* (m)

k_{fat} – *Thermal conductivity of adipose tissue* $\left(\frac{W}{m \cdot K}\right)$

k_{skin} – *Thermal conductivity of skin tissue* $\left(\frac{W}{m \cdot K}\right)$

k_{sock} – *Thermal conductivity of DAE sock* $\left(\frac{W}{m \cdot K}\right)$

Nu – *Nusselt number*

Re – *Reynolds number*

D_H – *Hydraulic diameter* (m)

D_o – *Outer diameter of airflow channel* (m)

D_H – *Inner diameter of airflow channel* (m)

V – *Airflow velocity* $\left(\frac{m}{s}\right)$

$v\ -\ Kinematic\ viscosity\ \left(\frac{m^2}{s}\right)$

$P\ -\ Power\ consumed\ by\ the\ water\ heater\ (W)$

$I\ -\ Current\ (Amps)$

$R\ -\ Resistance\ (Ohms)$

LIST OF ACRONYMS

ADAM – Advanced Automotive Manikin

BMI – Body Mass Index

DAE – Dynamic Air Exchange

LCG – Liquid Cooling Garment

NASA – National Aeronautics and Space Administration

PCM – Phase Change Material

PVC – Polyvinyl Chloride

RH – Relative Humidity

SD – Secure Digital

SoC – Standard of Care

INTRODUCTION

Lower limb amputees are often dissatisfied with the comfort of their prosthesis. A recent literature review of 38 selected studies revealed that more than 53% of people with amputation experienced heat and/or perspiration discomfort inside their prostheses [1]. One of these studies described a survey of 90 lower limb amputees where 72% of participants reported that the most common cause for a "moderate or worse" reduction in their quality of life during the heat of summer was due to elevated skin temperatures and perspiration levels within the prosthetic socket and liner [2]. With an issue this prevalent, it is necessary to find new methods and materials that will aid in reducing thermal buildup and increase moisture transport away from the body.

Current prosthetic liners are usually made from silicon, polyurethane or a combination polymer with a fabric outer layer and have thermally insulating properties. Liners gently adhere to the skin and act as an interface between the skin and socket to provide stability and distribute weight bearing loads more evenly. A 2007 study [3] detailing the thermal conductivities of twenty-three different liners of varying material compositions found that even the best performing liner had a thermal conductivity coefficient of 0.266 W/m·K. This same study also noted that a typical lower limb prosthetic socket of plastic or carbon fiber layup adds an additional layer with a thermal conductivity coefficient in the range of 0.148 to 0.150 W/m·K. Low conductivity issues are compounded by the poor liquid permeability and breathability of the enveloping liner and socket.

Lack of liner breathability and permeability causes disproportionate amounts of moisture to pool against the skin. Although it is known that increased moisture content in skin increases skin friction somewhat [4–6], there is a threshold beyond which excessive moisture causes friction to decrease significantly and can prompt loss of adherence between skin and liner. Limb to liner adherence failure places the amputee in a dangerous and potentially embarrassing situation because the prosthesis may fall off the residual limb. Current methods for dealing with accumulated sweat are limited. Options like antiperspirants or simply doffing the prosthesis and drying the limb and liner buy the user some time, but antiperspirants may cause skin irritation while removing the limb over and over can be impractical and/or socially awkward. Low-dose Botulinum Toxin (Botox) injections significantly reduce perspiration [7] and need only be applied periodically. But, injections require an invasive procedure that could cause pain, hematoma at the injection site, mouth and olfactory tract dryness, and optical problems [1].

A study has shown that even small increases in activity, such as walking, can elevate skin temperature one or more degrees Celsius over normal resting temperatures [8]. This increase is aggravated by the insulating environment [9] created by the liner and socket that comprise a

typical suspension system. The body's response to elevated skin temperature is vasodilation and increased stimulation of the sweat glands [10]. Vasodilation increases blood flow to the periphery of the limb in an attempt to dump more heat from the system. The combination of increased skin temperature and friction along with lingering moisture in contact with the skin can lead to blisters and/or maceration [1].

Another element playing a key role in prosthesis comfort is user perception. Although increasing the heat removal rate from the limb in any amount would be beneficial, the user's perception of heat removal (i.e., perceived change in skin temperature) is what improves prosthesis comfort and results in prolonged use. One study showed that there is an inverse relationship between the starting skin temperature and the temperature differential required in order to perceive that heating or cooling is occurring [3]. User perception of thermal comfort is of key importance, then, in achieving the goal of increased activity level with the prosthesis. There is a direct correlation between socket comfort and prosthesis use [11]. Without the prosthesis, mobility and activity levels will be reduced.

There are various designs that have been developed and tested to remove heat from, or lower skin temperature for a body in an insulative environment (e.g., insulative clothing or a prosthesis). Recent methods utilize cooling mediums such as Phase Change Material (PCM) in the liner [12], water in liquid cooling garments (LCG's) [13–15], thermally conductive pathways embedded in the socket wall linked to a heat sink [16], airflow through channels in the socket wall [17], and a dynamic air exchange (DAE) socket where air is drawn through a thin sock between the skin and liner by a vacuum pump.

In 2014, Ohio Willow Wood (Mt. Sterling, OH, USA) introduced the Alpha® SmartTemp liner [12] which uses heat absorbing properties of the Outlast® (Outlast Technologies, Golden, CO, USA) PCM to slow the onset of skin temperature increase during elevated activity. A PCM works such that, as the limb produces more heat during increased activity, some of the PCM will melt and thereby absorb heat rather than reflect it back to the skin. However, due to the finite amount of PCM in the liner, there is a physical limit as to how much heat can be absorbed. Once this threshold is reached the liner will function the same as any other liner until an external cooling source resets the PCM's heat absorbing property. This seems likely to succeed in postponing the onset of heightened skin temperatures if there is a sufficient amount of PCM. But, once all of the PCM has undergone phase change, it can no longer absorb heat and would begin to reflect heat like a typical liner. Only after being cooled by other means could the PCM change back to solid form and regain its heat absorbing ability. Although PCM in liners is relatively new, a recent clinical trial [18] where 16 subjects cycled on a stationary bike for 25 minutes and rested 10 minutes showed reduced mean skin temperatures and perspiration when comparing a PCM liner to a non-PCM liner.

Liquid cooling garments (LCG's) are another concept that has been explored for use in controlling skin temperature. NASA has worked extensively on LCG's, to protect astronauts from excessive heat stresses during space walks, launch, and re-entry [13]. LCG's circulate a pre-cooled liquid through a circuit of small tubing embedded in the suit which is in contact with the skin. In this way, the high heat capacity of water can take advantage of both conductive and convective cooling. Scaling down a full body LCG for use on an amputee's residual limb would improve amputee comfort. However, the weight of the liquid and necessary circulation system would impede an amputee's ability to be active. The best solution will deliver cooling to the residual limb, remove moisture buildup caused by perspiration, and avoid the use of heavy liquid cooling components, while allowing the amputee to keep the limb attached.

Heat sinks are commonly used for dissipating large heat loads quickly by using a highly conductive material and increasing surface area. A study earlier this year applied this concept in a design analysis for a new cooling prosthesis [16]. The design uses heat pipes embedded in the socket to transfer heat energy to the heat sink and mounted cooling fan. Although heat transfer would be improved over a conventional socket, the liner would still impede heat flow between skin and heat sinks and reduce its effectiveness.

Utilizing the same concept cooling concept as a LCG, a new socket was developed using 3D printing (fused deposition modeling) to incorporate a helical channel in the socket wall [17]. As small pump forces air at approximately 2.8 L/m through the channel to remove heat from the limb by convection. Although effective cooling is shown, the presence of the helical channel necessitates a much thicker socket wall than a typical socket.

A novel new DAE socket, being evaluated for this study, uses a small vacuum pump and pressure sensor to dynamically maintain a slight vacuum in the socket while drawing moisture out a port in the prosthesis' distal locking pin. The vacuum increases holding power because pressure inside the socket is less than atmospheric pressure and creates a slight suction between the socket and limb. Powered by a standard 9V battery, the DAE uses a thin sock worn between the liner and skin that allows flow of air and moisture. Air enters the sock layer through four symmetrically radially spaced ports in the proximal end of the socket. It then flows through the thin sock layer and exits through the custom locking pin. The combination of sweat removal, potential evaporative and convective cooling, and slight vacuum hold could increase amputee comfort and activity level.

This research will explore several thermal regulation parameters to see what affect they have on residual limb skin temperature as well as the potential for latent and sensible heat removal. Analysis will (1) use a computational model to show how skin temperatures vary in different thermal environments, (2) compare the computational model to a physical test unit (thermal manikin), and (3) demonstrate some practical outcomes drawn from preliminary human subject

study results (n=2) that compare adherence between the DAE socket and a standard of care (SoC) pin lock socket.

METHODS

Despite the varied and creative approaches that have been explored for cooling all or part of the human body, an effective and usable solution for transtibial amputees has yet to be reached. In order to better understand and address this issue, the author will (1) develop a simple, computational heat transfer model representing the DAE socket, (2) validate the model with results from the manikin, and (3) implement a series of subject tests to assist in understanding the physical implications of the data from our model and manikin. The overall aim of this research is to better understand what variables can be manipulated in a prosthetic system and how their variation effects outcomes related to thermal and physical comfort.

COMPUTATIONAL THERMAL MODEL

BACKGROUND

Thermal models are a useful tool for exploring variable spaces more efficiently but not necessarily for predicting exact conditions. The purpose of this thermal model is to simplify exploration of the variable space and shed light on which variables have the greatest effect on lower limb cooling, as well as to quantify the effect. Many physiological thermal models in existing literature represent body heat flow characteristics in great detail. With finite element analysis or detailed 2D thermal representations, decently accurate skin temperature predictions have been achieved. A 1997 study demonstrates that skin temperatures can be predicted with reasonable accuracy for a range of ambient temperatures often experienced by humans. It uses a six-cylinder model to approximate different portions of the body [19]. A more recent publication demonstrates a physiological model that helps predict thermal comfort in non-uniform transient thermal environments [20]. Although often precise, the high level of detail and knowledge of key information required to make these models work can be a hindrance to intuitive understanding of the problem. This approach aims to intuitively demonstrate the qualitative and approximate quantitative effect of certain variables on the performance of the system as a whole.

APPROACH

Computational model testing aims to observe the effect of air flow velocity, air flow temperature, ambient air temperature, and relative humidity of ambient air on heat removal. These results will then guide selection of tests to be performed on the thermal manikin. Utilizing a computational model to guide benchtop testing minimizes the associated time costs while yielding the most pertinent data. It may also allow the researcher to estimate the results of a change (e.g., installing a larger pump to increase air flow) before making changes to a design.

This model uses iterative solving to calculate the heat energy added to the system from the amputee's limb. It assumes a long insulated channel with a thin, continuous layer of sweat on the skin. A stream of air with known specific humidity and temperature enters at the proximal end of the socket. Specific humidity and temperature of the exiting air flow must also be known. However, for simplicity, exiting air will be assumed to be fully saturated (i.e., the relative humidity is 100%) due to sweat evaporation. Monitoring the mass flow rates of dry air and water vapor at entrance and exit, as well as the mass flow rate of sweat, allows for calculation of heat energy transferred through evaporation and convection.

The liner and socket were assumed to form an adiabatic insulating outer boundary and, therefore, heat loss to the environment through conduction was ignored. Radiation heat transfer was also considered negligible under the assumption that physical test data, collected for comparison, would be gathered inside a building with no significant incoming or outgoing heat radiation.

Because model validation was performed by benchtop testing the thermal manikin, model parameters were set to match its characteristics. Table 1 lists the measurements used to define the manikin shape. Surface area for each section of the manikin was calculated using the formula for a conical frustum. Surface area for the most distal section was calculated for a cone defined by $y = x^{1.1725}$ on the interval from 0 to 0.102 meters. The curve fit is based on measurements for the most distal section of the manikin. All values were summed for a total surface area, $A_s = 0.181\ m^2$. The radius was determined for an equivalent cylinder with the same length, $L = .406\ m$, and surface area as the manikin. Radius for this cylinder was found with

$$r_i = \frac{A_s}{2\pi L} \tag{1}$$

which yields a value of $r_i = 0.071\ m$. The sock between the leg and liner has a thickness of 1.5mm. An outer radius is defined as the radius of the leg plus the thickness of the sock layer, $r_o = .0725\ m$. The cross-sectional area for air flow can be defined as

$$A_{cs} = \pi(r_o^2 - r_i^2) \tag{2}$$

Volumetric flow rate (m^3/s) can be found as

$$\dot{V} = A_{cs}V \tag{3}$$

with V as the velocity of the air flow through the sock layer against the skin (m/s). Mass flow rate of dry air can be defined as

$$\dot{m}_a = \rho_a \dot{V} \tag{4}$$

where the density of dry air (kg/m^3) is

$$\rho_a = \frac{P_{atm}}{RT_{avg}} \tag{5}$$

The specific gas constant for air is $R = 287.05$ (J/kg·K), atmospheric pressure is $P_{atm} = 101325$ (Pa), and T_{avg} is the average temperature of the air (K) inside the socket.

Energy transfer between the body and the forced airflow through the socket was determined using the laws of conservation of energy and mass. The system is defined as the gap between the skin and the liner. First, consider the energy balance

$$\dot{E}_{in} + \dot{Q}_{in} + \dot{W}_{in} = \dot{E}_{out} \tag{6}$$

where $\dot{E}_{in}$ is the internal energy added to the system (W). Because flow velocity wouldn't vary significantly in practice and potential energy change is very minimal, changes in kinetic and potential energies of the airflow are assumed to be negligible. $\dot{Q}_{in}$ represents the heat energy being added to the system (W). Positive values indicate heat flowing from the body to the air, while negative values indicate heat flowing from the air to the body. There is no mechanical work being done. Therefore, $\dot{W}_{in} = 0$. $\dot{E}_{out}$ is the total energy leaving the system (W).

Applying the law of conservation of mass produces two more equations. The first

$$\dot{m}_{a_1} = \dot{m}_{a_2} = \dot{m}_a \tag{7}$$

states that the mass flow rate of dry air entering the system, m_{a_1} (kg/s), is equal to the mass flow rate of dry air exiting the system, $\dot{m}_{a_2}$ (kg/s). For simplicity they are lumped into a single term, $\dot{m}_a$ (kg/s).

The second equation

$$\dot{m}_{w_1} + \dot{m}_f = \dot{m}_{w_2} \tag{8}$$

demonstrates that the sum of the mass flow rate of water vapor entering the system through airflow and sweat evaporation, $\dot{m}_{w_1}$ (kg/s) and $\dot{m}_f$ (kg/s) respectively, is equal to the mass flow rate of water vapor exiting the system in the airflow, $\dot{m}_{w_2}$ (kg/s). Note that the mass flow rate of fluid (i.e., sweat) into the system could be a limiting factor based on the sweat rate of the amputee for a given set of conditions.

Using the definition of specific humidity, equation (8) can be rewritten as

$$\dot{m}_f = \dot{m}_a(\omega_2 - \omega_1) \tag{9}$$

using ω_1 and ω_2 as the specific humidities (kg/kg) of the entering and exiting air streams respectively. They can be calculated as

$$\omega_2 = \frac{0.622P_v}{P_{atm} - P_v} \tag{10}$$

and

$$\omega_1 = \frac{0.622\varphi P_g}{P_{atm} - \varphi P_g} \tag{11}$$

Atmospheric pressure is at sea level such that, $P_{atm} = 101325$ (Pa). Vapor pressure is represented by P_v (Pa) and calculated, for equation (10), at the exiting air temperature, T_2. Saturated vapor pressure of water is represented by P_g(Pa) and calculated, for equation (11), at the entering air temperature, T_1.

The energy of the entering fluids (sweat and humid air) can be calculated as the product of the mass flow rate and the enthalpy of the fluid. Enthalpy depends on the temperature and phase state of the fluid and can be looked up in a table. For this model, energy flow into the system is

$$\dot{E}_{in} = \dot{m}_a h_1 + \dot{m}_f h_{f_2} \tag{12}$$

and energy flow out is

$$\dot{E}_{out} = \dot{m}_a h_2 \tag{13}$$

h_1 and h_2 are the total enthalpies of humid air (kJ/kg) at temperatures T_1 and T_2 respectively. Similarly, h_{f_2} is the enthalpy (kJ/kg) of water at the outflow temperature T_2. It is assumed that outflow temperature at system equilibrium is equal to the skin temperature.

Rearranging equation (6) and substituting in equations (12) and (13) yields

$$\dot{Q}_{in} = \dot{m}_a h_2 - (\dot{m}_a h_1 + \dot{m}_f h_{f_2}) \tag{14}$$

representing the total increase in energy of the system due to heat flow. Equation (14) can be expanded further by expressing h_2 and h_1 as sums of the enthalpies of dry air and of water vapor. Heat loss is assumed to occur only through evaporation and convection from airflow in the sock

layer. Note that sensible heat transfer comes from convection of energy in the fluid and latent heat transfer from advective mass transfer of water vapor. Convection of energy is a combination of diffusion and advection where advection is defined as the transfer of energy, or enthalpy, by the bulk flow of the fluid. Diffusion is the transfer of energy on a molecular level (i.e., conduction). Substituting equation (9) and simplifying produces

$$\dot{Q}_{in} = \dot{m}_a\big(c_P(T_2 - T_1) + \omega_2 h_{fg_2} - \omega_1(h_{g_1} - h_{f_2})\big) \tag{15}$$

The specific heat of dry air at constant pressure, $c_P = 1.005$ (kJ/kg·K), is used under the assumption that pressure in the system remains fairly constant. h_{fg_2} is the enthalpy of vaporization for water (kJ/kg) calculated at the outflow temperature of the air. Likewise, h_{g_1} is the enthalpy of water vapor (kJ/kg) at T_1, and h_{f_2} is the enthalpy of saturated water (kJ/kg) at T_2. Values for h_{fg_2} and h_{f_2} are determined by interpolation from published tables. In the temperature range from -10 to 50 °C, the enthalpy of water vapor in air can be taken to be equal to the enthalpy of saturated vapor at the same temperature [21]. It can be approximated with negligible error in this range as

$$h_g(T) \cong 2500.9 + 1.82T \tag{16}$$

where T is the temperature of the vapor in °C. Using equation (15) it is possible to determine the heat energy transfer that occurs between the body and the dynamically exchanged air. For the iterative process it is then necessary to calculate a new outlet temperature (T_2) to replace the initial guess.

First, an equivalent thermal resistance consisting of conduction across adipose and skin tissues as well as the convective resistance from the skin to the air must be determined. This is simply the sum of the resistances represented by

$$R_{eq} = R_{tissue} + \frac{1}{h_c A_s} \tag{17}$$

where R_{tissue} is the lumped thermal resistance value for adipose and skin tissue (K/W). It was approximated to be

$$R_{tissue} = \frac{1}{A_s}\left(\frac{t_{fat}}{k_{fat}} + \frac{t_{skin}}{k_{skin}}\right) \tag{18}$$

using averaged values for the thickness of adipose and skin tissues as $t_{fat} = 3.65\ (mm)$ and $t_{skin} = 2.01\ (mm)$ respectively [22]. Values for the thermal conductivity of fat and skin have

been previously found to be $k_{fat} = .219\ \left(\frac{W}{m \cdot K}\right)$ and $k_{skin} = .498\ \left(\frac{W}{m \cdot K}\right)$ respectively [23]. Because the thickness of these tissue layers is so small, the surface area of each is approximated as equal to that of the skin.

The convective heat transfer coefficient, $h_c\ \left(\frac{W}{m^2 \cdot K}\right)$, is well known to be difficult to determine in practice. However, using the definition of the Nusselt number it can be calculated as

$$h_c = \frac{Nu \cdot k_{sock}}{D_H} \tag{19}$$

where Nu is the unitless Nusselt number, $k_{sock} = .0364\ \left(\frac{W}{m \cdot K}\right)$ being the thermal conductivity of the sock layer [23], and D_H is the hydraulic diameter (m) of the equivalent cylinder. For flow through a concentric annulus, the hydraulic diameter simplifies to be the difference of the outer and inner diameters of the annulus

$$D_H = D_o - D_i = .0024\ m \tag{20}$$

The Nusselt number is a ratio of convective to conductive heat transfer across a boundary, normal to the surface. Since the outer boundary (i.e., the liner and socket) is adiabatic it can be ignored. For the skin boundary the Nusselt number can be considered a constant ($Nu = 4.86$) for a concentric annulus with an inner to outer diameter ratio near one and a constant inner surface temperature [24]. This holds true only for laminar flow, namely a Reynolds number below 2300.

$$Re = \frac{V D_H}{\nu} \tag{21}$$

The DAE pump produces a maximum volumetric flow rate $\dot{V} \approx 1.4\ \left(\frac{L}{min.}\right)$. The cross-sectional area for airflow between the limb and liner is $A_{cs} \cong 6.8x10^{-4}\ (m^2)$ which leads to a flow velocity of $V = 3.5x10^{-2}\left(\frac{m}{s}\right)$. Assume a kinematic viscosity for dry air of $\nu = 1.62x10^{-5}\ \left(\frac{m^2}{s}\right)$ at a temperature of 30 °C. Note that this will be a reasonably close estimate as the water vapor, even at 100% relative humidity, will only account for a couple percent of the humid air mass as dictated by the specific humidity. Reynolds numbers range from $Re = 5.1$ for current DAE flow to $Re = 74.1$ for $V = 0.5\ \left(\frac{m}{s}\right)$. Both values are well below the turbulent transition threshold.

Finally, the maximum outlet temperature reached at equilibrium, T_2 (K), can be calculated from

$$T_2 = T_{core} - Q_{in} R_{eq} \tag{22}$$

A value for the body's core temperature, $T_{core} = 310.85\ K$, was chosen based on findings about the intravascular temperatures of legs in men during submaximal exercise [25].

Summary of model assumptions:

1. Leg geometry is represented by an equivalent cylinder.
2. Fully developed laminar flow.
3. Fully developed thermal boundary flow.
4. Constant core body temperature at 310.85 K.
5. Adiabatic outer boundary (liner and socket).
6. Kinetic energy change between inlet and outlet flow is negligible.
7. Potential energy change between inlet and outlet flow is negligible.
8. Sock layer is represented by an air gap between the skin and liner.
9. Skin surface is completely and uniformly coated with sweat.
10. Socket radiates and absorbs negligible energy from lab surroundings.
11. Radiation heat transfer to or from the skin is negligible.
12. Outflow air is saturated (i.e., RH=100%).
13. Outflow air temperature is calculated at system equilibrium.
14. Outflow temperature is equal to sweat and skin surface temperature.
15. Pressure is constant (atmospheric pressure for standard conditions at sea level).

THERMAL MANIKIN

BACKGROUND

A thermal manikin is a device that mimics the human body's thermal response to the environment through temperature control, and allows for iteration of design parameters more rapidly than is feasible with human subjects. Manikins have been made of many materials including copper, aluminum, plastic, and specialized fabrics. These manikins may be full-body or just a section such as a limb.

Chauncy, the name given to one of the first thermal manikins, was built in the late 1940's at General Electric [26]. Its purpose was to aid development of better clothing for military personnel who were serving in extreme conditions. The first female based manikin was developed in Denmark in 1989 [27]. Another more recent example is the ADvanced Automotive Manikin (ADAM) [28], which is an entirely self-contained unit that has the added ability to sweat. It has been used in test programs with NASA to evaluate the NASA Shuttle and Russian Orlan LCG's for astronauts and cosmonauts [14]. In an effort to increase automobile efficiency, ADAM was also used to test ventilated seats for more localized and effective cooling [29]. A more comprehensive look at thermal manikin history was performed in 2004 and mentions that over 100 thermal

manikins are in service worldwide [30]. Thermal manikins have been proven effective and valid as an excellent starting point in developing physiological thermal control systems.

APPROACH

The thermal manikin, designed and constructed for measuring heat transfer during testing of novel prosthetic interventions [31], will be used to validate results from the thermal model described in the following section. ASTM standards were referenced as guidelines during the manikin's development [32–35]. In addition to these standards, details on construction material and heating methods used by other full body and limb based thermal manikins were considered to help guide in design. The shell was constructed from 1.5mm thick copper and sized using the radius dimensions in Table 1. For testing with the DAE socket, the manikin is first covered with a thin sock and then the liner. The "limb" is then placed in a typical plastic socket stand. Finally, the copper shell is filled with water up to a height equal with the proximal lip of the liner.

TABLE 1: DIMENSIONS USED IN CONSTRUCTING THE THERMAL MANIKIN

Distance from distal end (m)	.406	.330	.254	.178	.102	0
Radius (m)	.096	.091	.081	.072	.069	0
Surface Area (m^2)	.045	.041	.037	.034	.024	

Water inside the copper shell was heated and maintained at a constant temperature to simulate a body core temperature at 37 °C. Temperature control was accomplished with a PID controller (CT 16A, Minco Products Inc.) monitoring temperature with a J-Type thermocouple (Immersion Thermocouple, Type J, 3/16" Diameter, Thermo-Couple Products Co.) and heating with a 250 watt immersion cartridge water heater (EM37-5, HotWatt). A fish tank bubbler (Tetra Whisper10, Spectrum Brands Inc.) was used to mix the water and maintain an even temperature distribution throughout the limb volume. A 54mm thick, square of closed-cell foam was placed across the proximal opening as a seal to minimize heat loss from the top of the manikin. Wires for the heater and thermocouple, as well as the tube for the bubbler, were routed through small holes in the foam.

Current flow through the water heater was measured (MTX 3281, AEMC Instruments) to determine the power delivered to the system by the water heater. Power consumed by the heater is assumed to represent the heat removed through cooling. Conduction was considered negligible due to the insulative properties of the liner and socket stand and closed-cell foam.

Airflow through the sock layer was produced by a 6V vacuum pump (CTS-Series, Parker Hannifin, Hollis, NH, USA) connected to a barbed port (fits 1/8" ID tubing) on the distal end of the liner. Depending on moisture content of the sock, it can produce a volumetric flow rate of up to 1.4 L/min. Assuming the sock creates a 1.5 mm gap between the limb and liner, this volumetric flow

rate creates approximately 0.035 m/s uniform flow against the skin. The pump motor was driven by a motor shield (ArduMoto, SparkFun Electronics) mounted on a microcontroller (Uno, Arduino LLC). For testing, the microcontroller was powered with a DC power supply such that the pump motor received 7.7V (the motor is intentionally overdriven). This replicates conditions for the DAE socket with a fresh 9V battery.

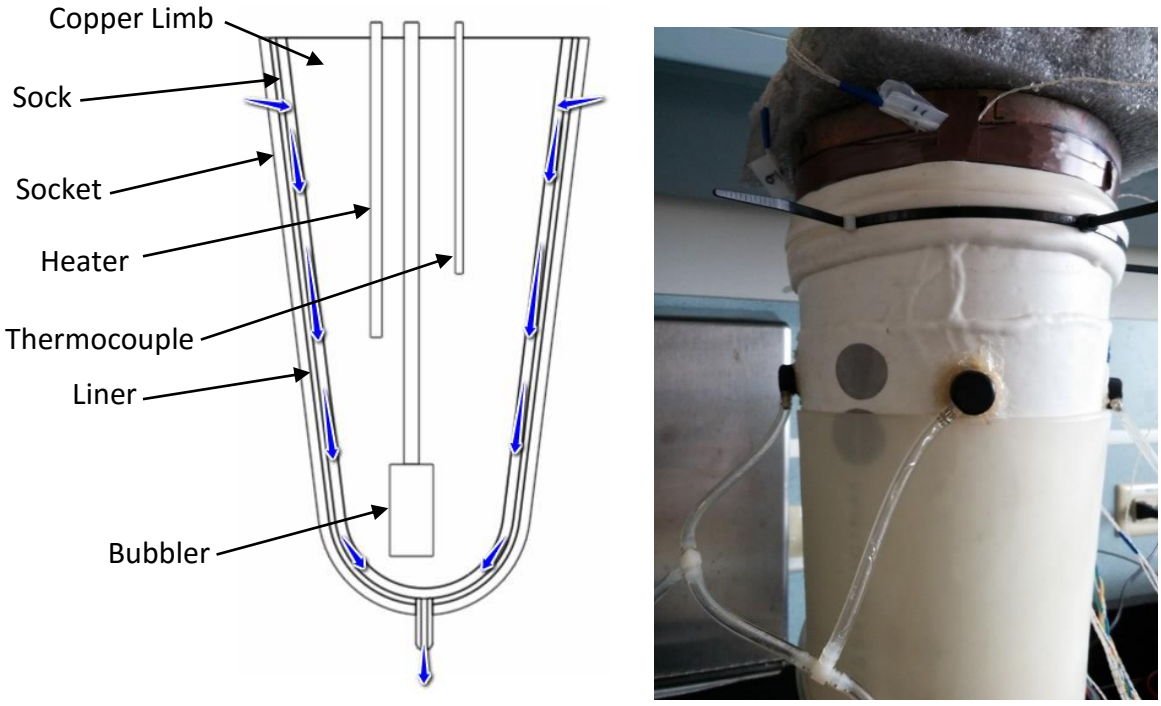

FIGURE 1: (LEFT) THE THERMAL MANIKIN SHOWING THE COPPER LIMB WITH THE SOCKET, LINER, AND SOCK CUT AWAY. AIR FLOWS THROUGH THE SOCK LAYER AND OUT THE DISTAL LOCKING PIN AS DEMONSTRATED BY THE BLUE ARROWS. (RIGHT) FULLY DRESSED THERMAL MANIKIN SHOWING THE SOCKET, LINER, PROXIMAL PORTS, COPPER SHELL, AND SQUARE FOAM TOPPER.

Three data loggers (SmartReader Plus 8, ACR Systems Inc.) gathered temperature measurements from eighteen 2-wire, negative temperature coefficient thermistors (MA-100, ThermoProduct, Co.). Twelve thermistors were affixed directly to the outside of the copper shell using small pieces of electrical tape. Care was taken not to tape over the thermistors as this would lead to increased insulation and increase measurement error. Thermistors were placed in four columns containing three thermistors each (proximal, mid, distal). They were evenly spaced around the circumference of the shell in anterior, lateral, posterior, and medial positions. The proximal thermistors were located directly under the air inlet ports, the distal thermistors were approximately two inches from the tip of the limb, and the middle thermistors were halfway between their distal and proximal neighbors (Figure 2).

FIGURE 2: THERMISTOR PLACEMENT ON THERMAL MANIKIN.

Next the thin sock was rolled up over the manikin shell and four additional thermistors were taped to the outside of the sock directly over other middle thermistors. The goal was to measure temperature on the path where airflow velocity was expected to be greatest due to the small inner diameter of the inlet tubing.

TEST PROTOCOL

The thermal manikin's purpose is to physically test the DAE socket without need of a human participant. Power consumption of the water heater is the most useful metric for monitoring heat removal from the manikin. Skin, liner, and ambient air temperatures are measured for comparison with the computational model. Temperature readings, although not vital to analysis, help determine the temperature gradient magnitudes driving heat transfer within the socket. Heat removal rates are compared to estimates from the computational model.

Test cases for the manikin are as follows:

1. Dry sock, passive air flow
2. Dry sock, active air flow
3. Wet sock, passive air flow
4. Wet sock, active air flow

Passive air flow represents idle conditions (i.e., no forced flow, pump is inactive). Active air flow represents forced flow in the system when the pump is continuously active. Each of the four conditions was tested three times for 30 minutes each. For test cases three and four, wetting the sock was achieved by forcing water in through the distal port until a steady stream could be seen

from all four of the proximal ports. Standing water was then pumped out of the sock and the system temperature was allowed to stabilize before beginning data collection.

Average power consumption of the water heater was recorded for each test and averages were calculated within each condition. Convective cooling power was found by subtracting the dry passive power value from the dry active power value. Results were compared to those produced by the computational model to validate model results.

HUMAN SUBJECTS

APPROACH

Human subject research is used to determine what improvements (if any) a DAE socket, compared to the standard of care, will have on adherence duration among lower limb amputees during increased activity in warm, humid conditions.

Five hypotheses are tested in this study. They are as follows:

- *$H_{1.1}$ – The duration transtibial amputees can ambulate before loss of adherence will decrease with increasing environment temperature.*
- *$H_{1.2}$ – The duration transtibial amputees can ambulate will be longer while wearing the DAE system as compared to the SoC socket.*
- *$H_{2.1}$ – The amount of sweat when adherence is lost will be independent of environment temperature while wearing the SoC socket.*
- *$H_{2.2}$ – The amount of sweat expelled from the DAE socket will increase with increasing environment temperature.*
- *$H_{2.3}$ – The amount of sweat collected from the SoC socket will increase with increasing environment temperature when adherence is not lost.*

TEST PROTOCOL

Unilateral transtibial amputees were recruited to participate in this Institutional Review Board-approved study. Participants were 3 and 48 years, unilateral transtibial amputees, wore their prosthesis at least four hours per day, had been fitted with and using a prosthesis for at least six months, and able to walk on a treadmill at a brisk speed for 30 minutes at elevated temperature and humidity while maintaining heartrate below a set target (110 bpm on beta blockers, (220-age)*0.75 bpm for all others). Participants were asked to provide additional information that included: age, sex, weight, height. Weight and height were self-reported.

Each participant completed six test sessions, three wearing the novel DAE prosthesis (Figure 3), and three wearing a standard of care prosthesis. Both were fit by a certified prosthetist. The DAE

prosthesis included: a custom, thin textile sock with an elastomeric air seal on the proximal lip, a modified pin lock elastomeric liner with four proximally located occlusion preventing liner ports and a hole through the center of the distal locking pin (liner is similar to an Ossur Dermo (Foothill Ranch, CA, USA)), a total contact socket with a custom-designed, 9V-battery-operated negative gauge pressure producing pump and associated components attached to the socket exterior.

The DAE system uses a small vacuum pump (CTS Series; Parker Hannifin, Hollis, NH, USA) to produce a small proximal-to-distal pressure differential (~10 kPa) across the residual limb for increased adherence. A solenoid valve (High Density Interface solenoid valve; The Lee Company, Westbrook, CT, USA), which can be opened on demand by the user, allows air flow in through the four proximal ports. Flow continues through the sock weave to ventilate the user's skin and exits the modified distal locking pin. Depending on fit and moisture content of the sock, air flow may be up to 1.4 L/min. Air flow also enables expulsion of perspiration from the thin sock.

The SoC prosthesis included: an elastomeric liner (Alpha silicone; Ohio Willow Wood, Mt. Sterling, OH, USA), a total surface bearing socket. For both systems, a passive energy storing prosthetic foot (LP Vari-Flex with EVO; Ossur, Foothill Ranch, CA, USA) was attached to the aluminum pylon. The pylon mounted directly to the socket for the SoC, whereas the DAE had a custom manifold to catch expelled perspiration mounted between the pylon and socket. When needed, an additional wool or synthetic sock was worn exterior to the liner to improve socket fit. Participants were randomly assigned to begin the study with either the DAE or SoC prosthesis.

Participants were asked to walk on a treadmill in a chamber at 20, 30, and 35 °C with relative humidity at approximately 50% with each socket. Chamber temperature order was randomized for each of the two prostheses, per participant. Water was supplied for drinking and participants were encouraged to drink as much as they wanted during the test.

Participant walking speed was self-selected and determined by averaging four passes down the hallway. Participants could elect to make a slight initial adjustment to the treadmill walking speed that was then held constant for all six tests.

To replicate hot, humid conditions in the lab, a six by ten foot test chamber was built and a treadmill placed inside. The enclosure consisted of a wooden frame, made with two-by-four's, from which was hung a clear vinyl curtain that reached the floor. A ceiling was created with half inch foam insulation board. Gaps between the frame, curtain, and foam board were closed with tape.

Depending on the required temperature, one or two 1500 watt space heaters (EW6507L, DeLonghi and BH3950, Bionaire) and a humidifier (05521, Hamilton Beach) were used to condition the chamber. A small fan (HT900, Honeywell) circulated the air to achieve uniform

conditions throughout the test chamber. Care was taken not to aim flow directly at the subject as this would increase cooling and variably alter sweat output. Temperature and humidity were recorded via a microcontroller (Uno, Arduino LLC) using a dual function sensor (Honeywell HIH9121) mounted from the treadmill control panel about four feet above the treadmill deck.

The same setup (Arduino Uno and Honeywell HIH9121) was used for monitoring the DAE's outflow temperature and humidity. The sensor was sealed inside a small PVC "T" and connected in line with the air outflow tubing. Data was logged to an onboard micro SD card and the microcontroller was powered by a 9V battery.

Participants began each of the six sessions sitting inside the chamber pre-heated to test temperature. After 30 minutes sitting they transitioned to walking at their self-selected pace on the treadmill, still in the heated chamber. Walking was terminated after 30 minutes or when the subject lost confidence in socket adherence, whichever occurred first. If confidence was lost before 30 minutes had expired, total walking time was recorded and the subject was transferred to a chair in room temperature conditions (i.e., approximately 21 °C). They then sat for another 30 minutes to finish sweating and cool down.

For both sockets, pre-test dry weights were recorded (CPA324S, Sartorius) for three absorbent cloths, two pairs of gloves, and a two by two inch square of gauze. For the DAE additional pre-test dry weights were recorded for the sock, "T" connector with humidity sensor, manifold, exhaust tubing, and two cotton swabs. All items were placed in labeled, sealed containers for weighing. During the test, the gauze was secured approximately midway between the ankle and knee, on the anterolateral side of the intact limb, using an adhesive, watertight barrier (Tegaderm Film, 3M Corp.). Moisture collected on the intact limb was used to compare sweat levels between participants without influence from the prosthesis.

Upon completion of each session, all detachable wetted components (mentioned above) were placed in their respective plastic containers and sealed to minimize evaporative losses. With one absorbent cloth held under the limb to catch any drips, the liner was slowly reflected, limb and socket were wiped down with the other two absorbent cloths, and wet items were sealed in labeled containers. Items were weighed and post-test weights recorded. Weight of the collected moisture was found as the difference between pre- and post-weights.

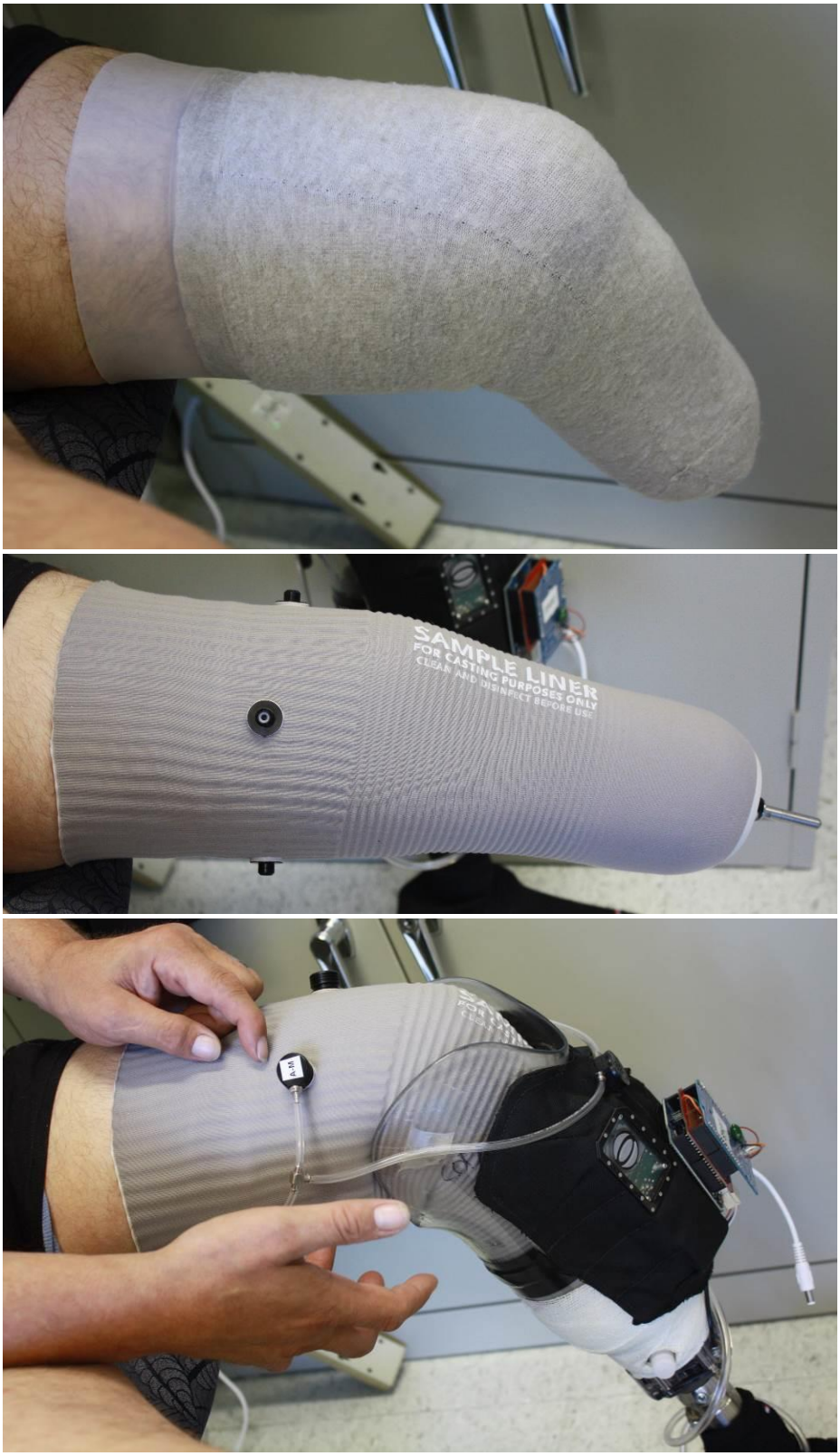

FIGURE 3: (TOP) CUSTOM SOCK WITH SILICONE SEAL ON THE PROXIMAL LIP. (MIDDLE) CUSTOM LINER WITH PROXIMAL PORTS. (BOTTOM) DAE SOCKET AND COMPONENT SLEEVE WITH THE MICRO-CONTROLLER FOR HUMIDITY AND TEMPERATURE SENSING.

FIGURE 4: LAYOUT OF THE TEST CHAMBER AS USED DURING SUBJECT TESTING

RESULTS

COMPUTATIONAL THERMAL MODEL

The output metric of primary interest from the computational model is heat flow rate. Effects of several variables including flow velocity, entering air temperature, and relative humidity are considered.

Increasing the flow velocity resulted in higher amounts of heat transfer (see Figure 5A, B, and C). At 20 °C and 50% RH, a flow velocity of 0.1 m/s transferred 6.0 W. Increasing flow velocity by a factor of four to 0.4 m/s resulted in more than tripling the heat transfer to 21 W. Changes in the ambient air RH also influenced heat transfer. At 20 °C and 10% RH,the heat transferred at a flow rate of 0.1 m/s was 50% greater than at 90% RH.

Change in heat removal per change in RH increased with ambinet air temperature. At 20 °C the difference in heat removal between 10% RH and 90% RH at 0.5 m/s is 9 W. At 35 °C the difference is 21 W.

A)

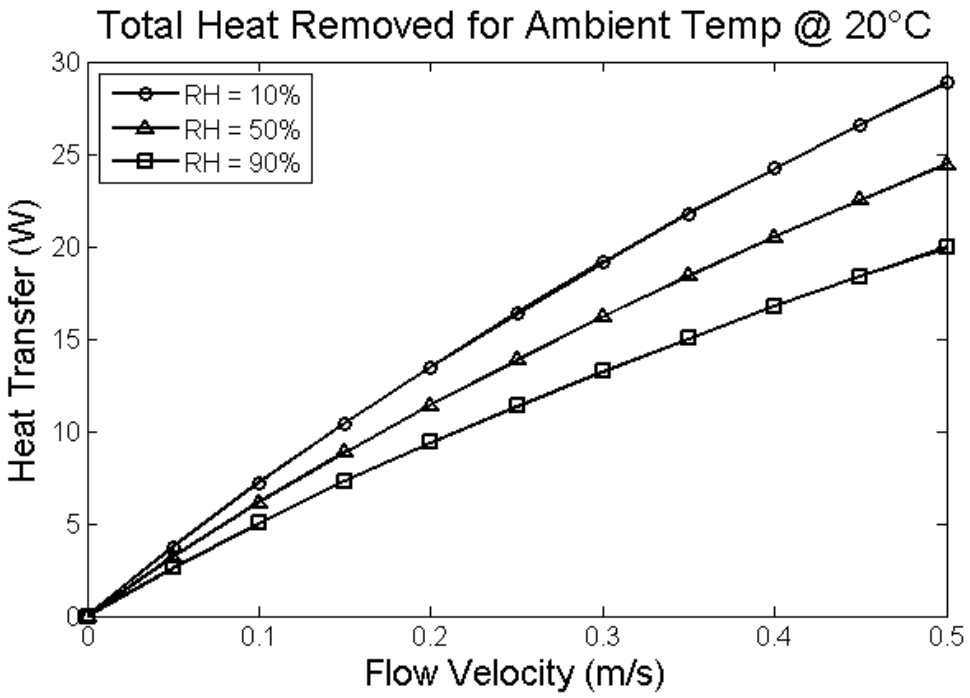
Total Heat Removed for Ambient Temp @ 20°C
RH = 10%
RH = 50%
RH = 90%
Heat Transfer (W)
Flow Velocity (m/s)
0
5
10
15
20
25
30
0
0.1
0.2
0.3
0.4
0.5

B)

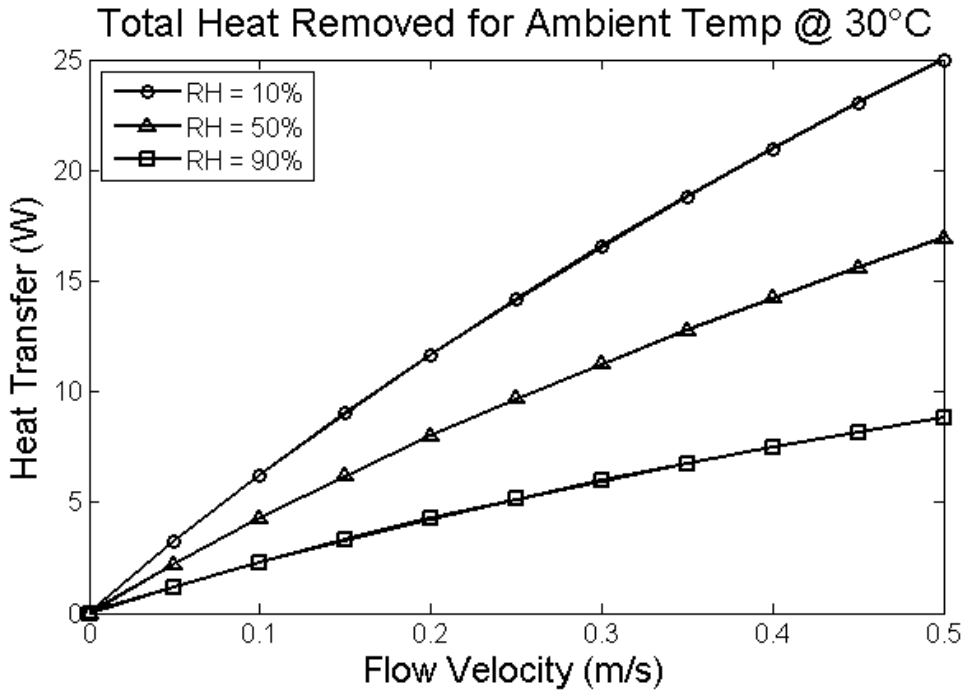
Total Heat Removed for Ambient Temp @ 30°C
RH = 10%
RH = 50%
RH = 90%
Heat Transfer (W)
Flow Velocity (m/s)
0
5
10
15
20
25
0
0.1
0.2
0.3
0.4
0.5

C)

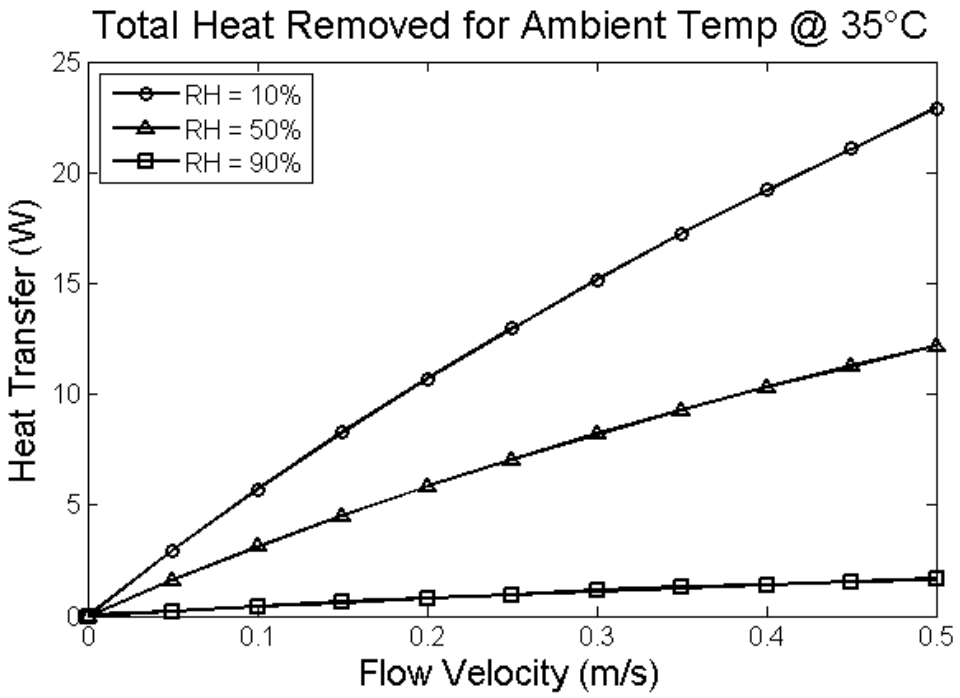

FIGURE 5: TOTAL HEAT REMOVED FROM THE BODY DUE TO DAE FOR (A) 20 °C, (B) 30 °C, AND (C) 35 °C FLOW INLET TEMPERATURES.

Another way to understand the effects of heat removal is by calculating the resulting changes in skin temperature (Figure 6A, B, and C). According to the model, skin temperature decreases with ambient air temperature. Skin temperature is 1.6 °C lower for air at 90% RH and a flow velocity of .25 m/s when comparing 20 °C ambient air conditions to 35 °C ambient air.

Skin temperature decreases with decreasing RH and airflow velocity. For 30 °C ambient air and a flow velocity of 0.1 m/s, a 0.8 °C increase in skin temperature occurs between the 10% and 90% RH conditions. For a 20 °C ambient air temperature at 10% relative humidity, skin temperature is predicted to decrease 4.8 °C between the no flow temperature and 0.5 m/s. No air flow (i.e., velocity = 0 m/s) results in skin temperatures equal to body core temperature. On the other extreme, 35 °C ambient air at 90% RH produces a mere 0.25 °C drop in skin temperature over the same 0.5 m/s flow rate range.

A)

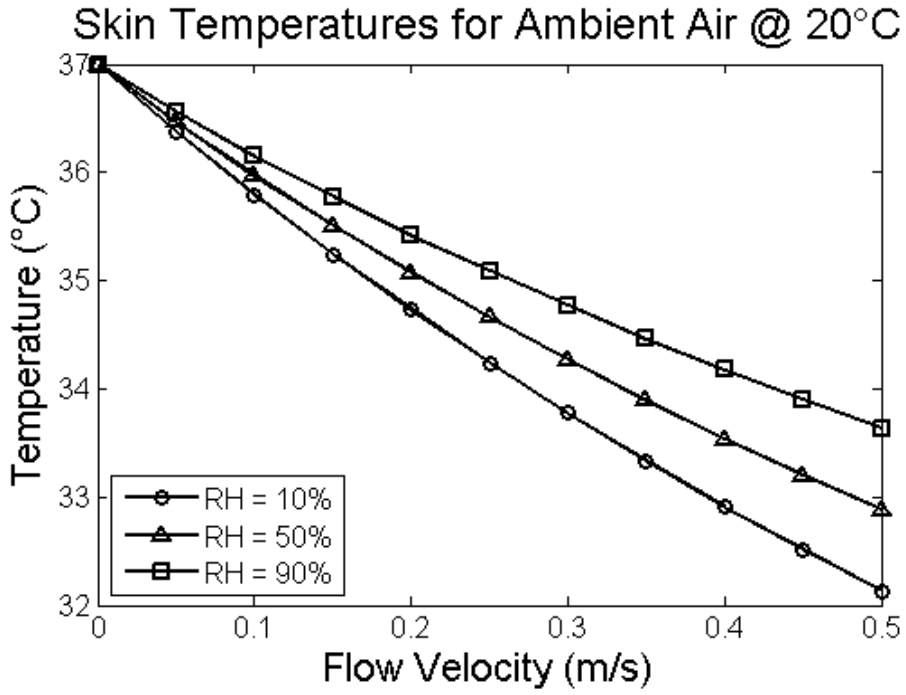
Skin Temperatures for Ambient Air @ 20°C
Temperature (°C)
Flow Velocity (m/s)
RH = 10%
RH = 50%
RH = 90%
37
36
35
34
33
32
0
0.1
0.2
0.3
0.4
0.5

B)

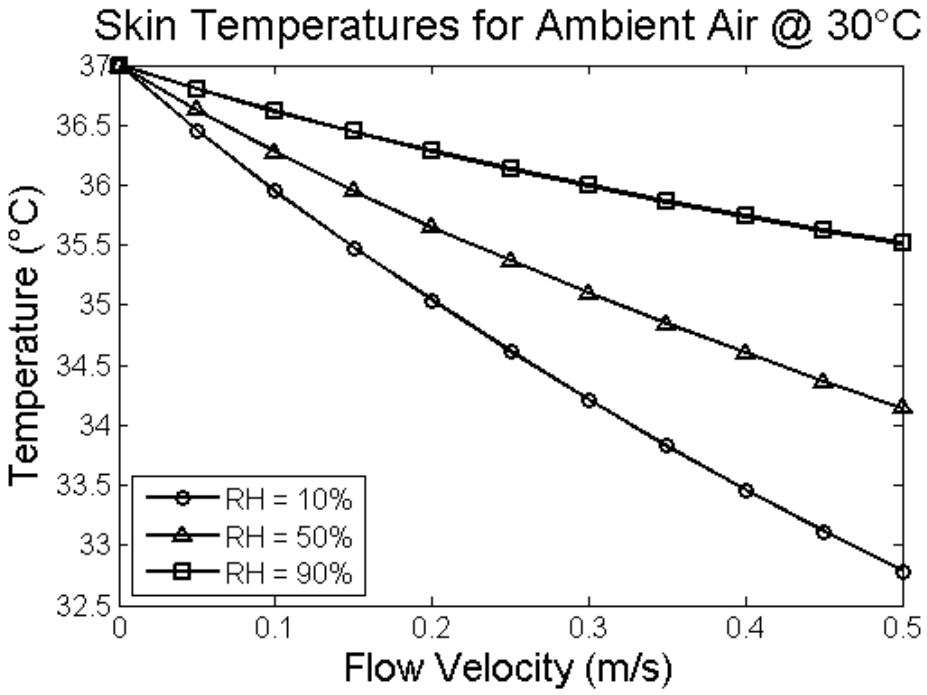
Skin Temperatures for Ambient Air @ 30°C
Temperature (°C)
Flow Velocity (m/s)
RH = 10%
RH = 50%
RH = 90%
37
36.5
36
35.5
35
34.5
34
33.5
33
32.5
0
0.1
0.2
0.3
0.4
0.5

C)

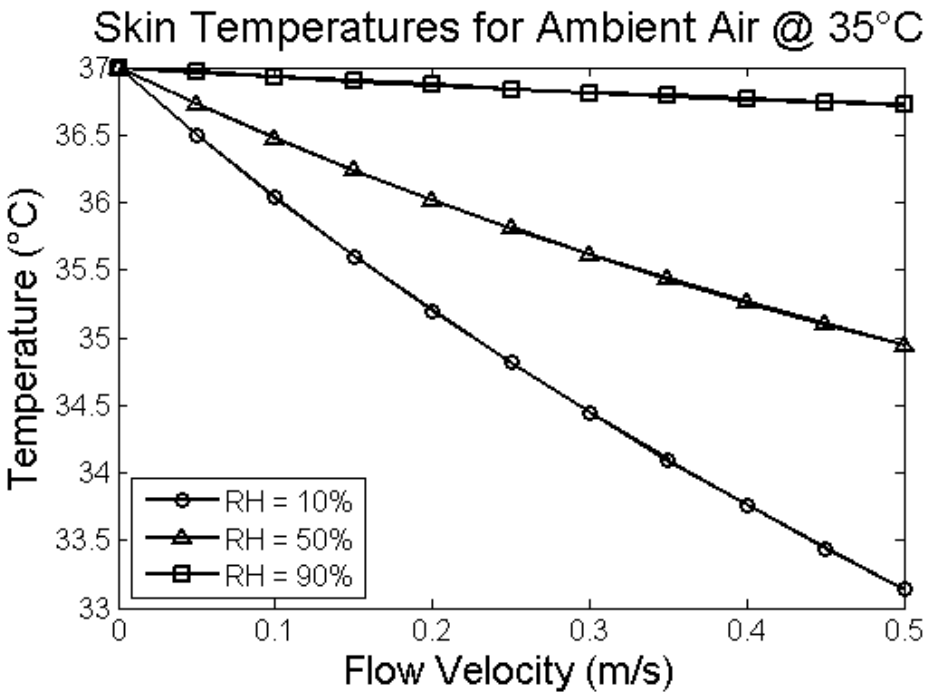

FIGURE 6: ESTIMATED SKIN TEMPERATURES FOR VARYING AMBIENT (INLET) AIR TEMPERATURES AND HUMIDITIES.

THERMAL MANIKIN

Neither case with the dry sock (passive or active pump) demonstrated any appreciable cooling during the 30 minute tests with the DAE setup (Figure 7A and B). Skin temperatures dropped less than 0.15 °C over the 30 minute test duration and liner temperatures behaved similarly. The wet sock with passive pump (Figure 7C) failed to produce appreciable cooling at the skin or the sock-liner interface. Temperature changes were more noticeable for the active flow through a wet sock (Figure 7D) and generated a maximum skin temperature decrease of 0.6 °C during a 30 minute test. Most skin temperature measurements showed a steady temporal decline resulting in an average drop of 0.3 °C over each of the three, 30 minute test spans. Inner liner temperatures declined in a linear fashion but saw no more than 0.3 °C of change.

A)

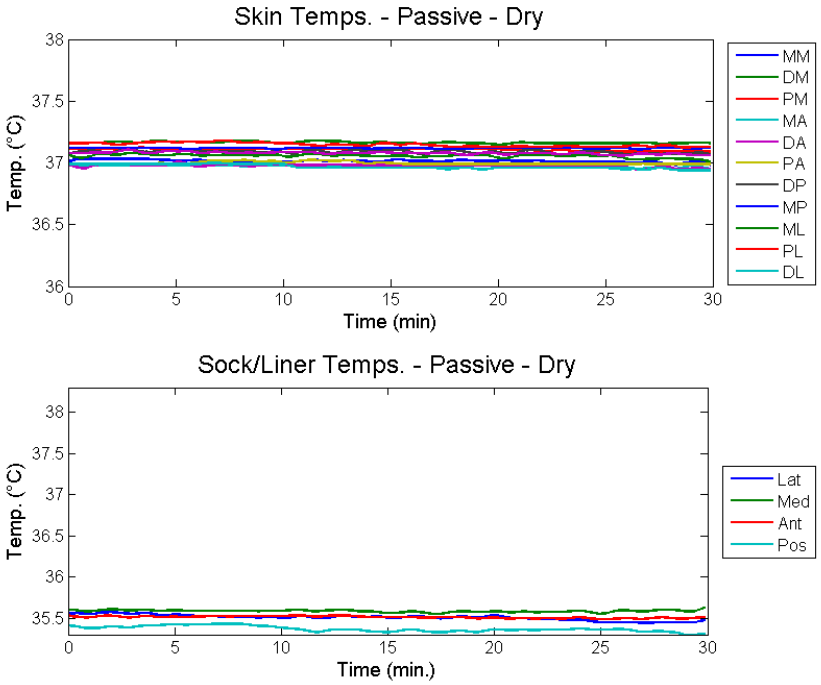
Skin Temps. - Passive - Dry
Temp. (°C)
Time (min)
MM
DM
PM
MA
DA
PA
DP
MP
ML
PL
DL
Sock/Liner Temps. - Passive - Dry
Temp. (°C)
Time (min.)
Lat
Med
Ant
Pos

B)

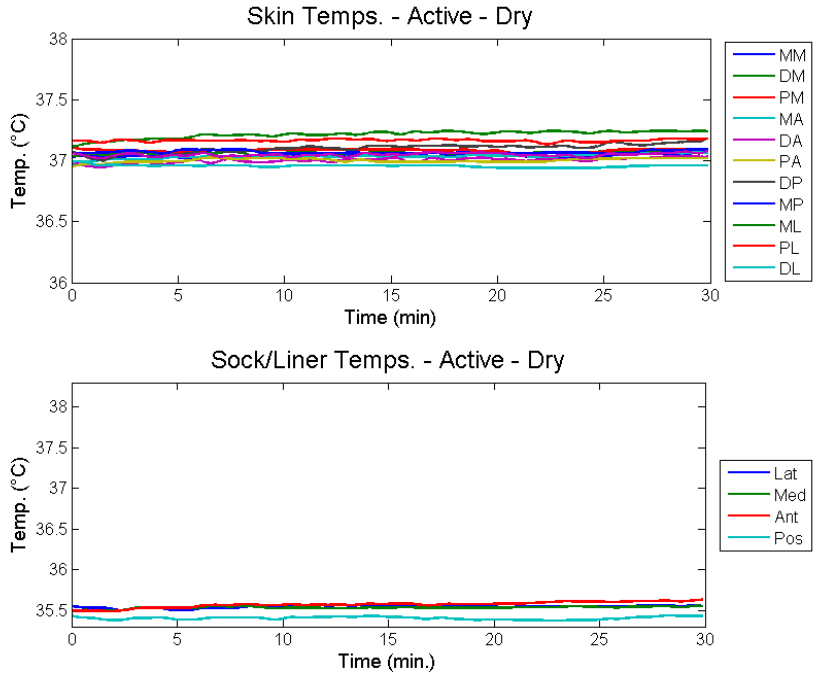
Skin Temps. - Active - Dry
Temp. (°C)
Time (min)
MM
DM
PM
MA
DA
PA
DP
MP
ML
PL
DL
Sock/Liner Temps. - Active - Dry
Temp. (°C)
Time (min.)
Lat
Med
Ant
Pos

C)

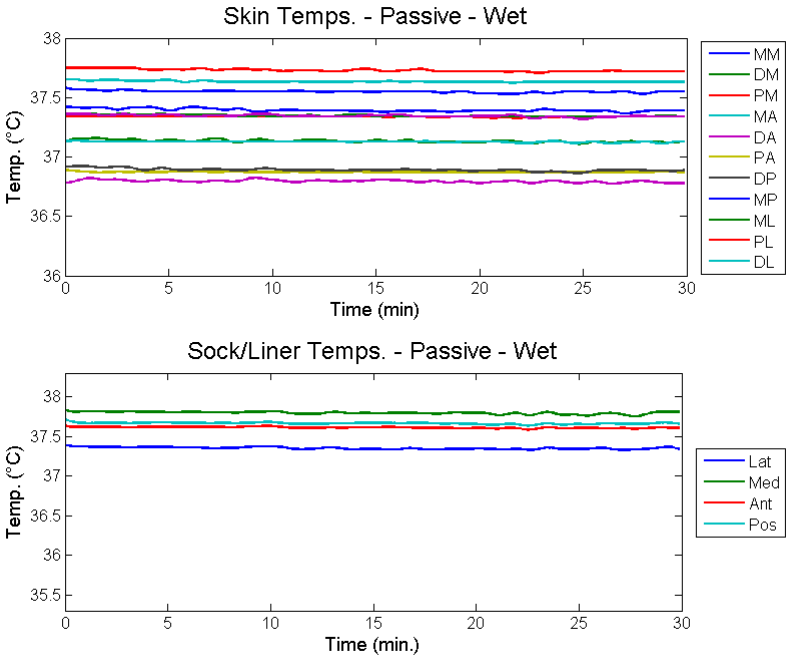

D)

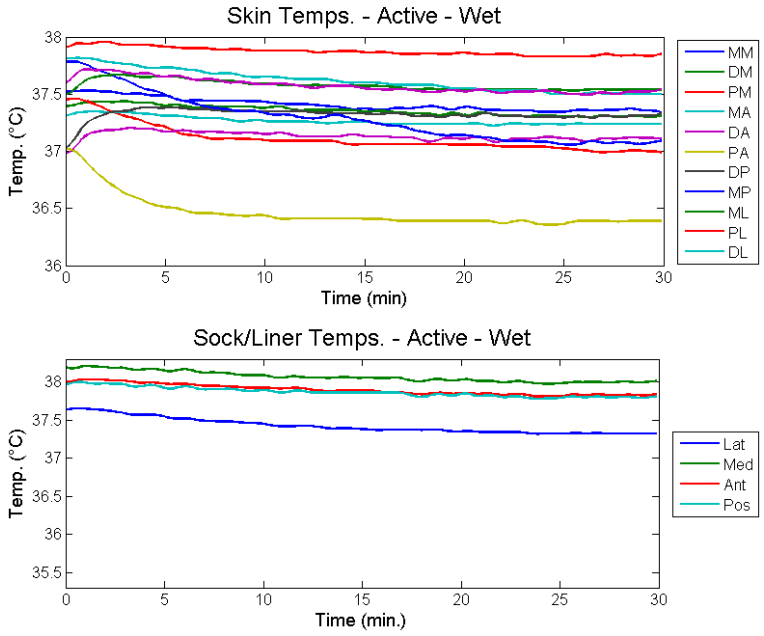

FIGURE 7: TEMPERATURES MEASURED ON THE THERMAL MANIKIN DURING EACH OF THE FOUR TEST CASES. IN THE SKIN TEMP LEGEND, THE FIRST LETTER DENOTES PROXIMAL (P), MID (M), OR DISTAL (D). THE SECOND LETTER DENOTES MEDIAL (M), LATERAL (L), ANTERIOR (A), OR POSTERIOR (P).

Average power consumed to maintain the water at body temperature was used to estimate the heat flow out of the manikin. Greater cooling occurred with a wet sock than dry for both active and passive cooling cases (Figure 8). Also, active cooling removed more heat for wet (21.8 W)

and dry (19.3 W) cases than their passive cooling counterparts (20.5 W for wet and 19.0 W for dry).

Forced convection and evaporation combined produce a 1.33 W cooling gain compared to natural convection and evaporation. Forced dry convection delivers a 0.27 W cooling increase compared to natural convection. The maximum benefit is delivered by combining evaporation and forced convection (DAE design) for a 2.77 W cooling advantage.

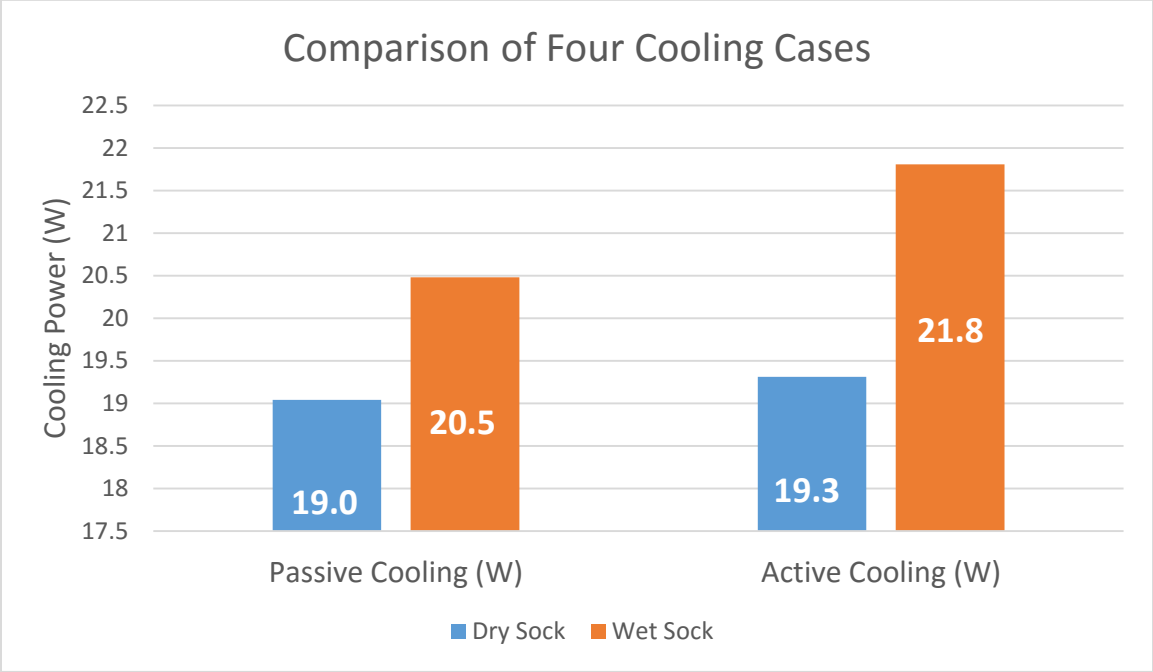

FIGURE 8: POWER CONSUMED BY THE WATER HEATER TO MAINTAIN WATER AT BODY TEMPERATURE IN A 21 °C ENVIRONMENT.

HUMAN SUBJECTS

Data presented for the human subject study are preliminary results. Due to the small sample size (n=2), inferential statistics cannot be used to draw any statistically significant conclusions. Both subjects were overweight and had worn a prosthesis for years (Table 2). Hypotheses can neither be confirmed nor rejected at this time. However, current results are presented with the assumption that the ongoing testing will bring statistical significance to early trends.

TABLE 2: PARTICIPANT CHARACTERISTIC INFORMATION

	Height (m)	Weight (kg)	BMI (kg/m^2)	Sex	Time since amputation (yrs.)	Etiology
Subject 01	1.80	86	26.5	M	21	Infection
Subject 02	1.75	111	36.2	M	9	Injury

The amount of sweat produced by each participant increases with chamber temperature, regardless of socket type (Table 3). For a given chamber temperature, sweat levels are consistently greater when participants are wearing the DAE socket than with the SoC. Adherence, the loss of which will be defined as an amputee's loss of confidence in the ability to ambulate safely without the prosthesis slipping off, does not seem to be effected when wearing the DAE socket. Although neither subject lost adherence during any test, Subject 02 experienced substantial pistoning and liner migration near the end of treadmill walking for both the 30 and 35 °C SoC tests.

$H_{1.1}$ states that loss of adherence will occur sooner with increasing environmental temperatures. Although Subject 02 did experience pistoning as well as proximal and distal liner slip for the 30 and 35 °C SoC tests, total confidence was not lost. The hypothesis cannot be confirmed nor rejected without further testing.

$H_{1.2}$ states that an amputee will be able to ambulate longer in a DAE socket compared to a SoC socket. However, both subjects completed the full 30 minutes of treadmill walking for all six chamber temperature and test socket combinations. Without an instance of adherence loss, the hypothesis cannot be confirmed nor rejected.

$H_{2.1}$ states that the amount of perspiration present when limb adherence is lost will be independent of environment temperature for the SoC socket. Only two of the 12 completed tests neared adherence loss. Sweat accumulation at the time of adherence loss shows a declining trend with increasing environment temperature. This neither proves nor disproves that environment temperature and sweat levels at adherence loss are independent of each other.

$H_{2.2}$ states that the amount of perspiration removed by the DAE system will increase with environment temperature. Sweat amounts averaged 1.57 g (±0.96 g) at 20 °C, 5.42 g (±0.77 g) at 30 °C, and 12.52 g (±2.88 g) at 35 °C. This increasing trend points to validation of the hypothesis.

$H_{2.3}$ states that the amount of perspiration in the SoC socket at test end (or loss of adherence) will increase with environment temperature. Sweat amounts averaged 0.08 g (±0.02 g) at 20 °C, 1.46 g (±0.17 g) at 30 °C, and 2.93 g (±1.46 g) at 35 °C. This increasing trend points to validation of the hypothesis. However, Subject 02 did see a decrease in collected perspiration from the 30 °C condition to the 35 °C condition.

TABLE 3: COLLECTED PERSPIRATION RESULTS OF PARTICIPANTS PRESENTED IN ORDER TESTED.

	Room Temp. (°C)	Socket Type	Total Sweat from Residual Limb (g)	Sweat from Intact Limb (g)	Time to Loss of Adherence (min.)	SSWS (km/h)	Duration (min.) Sit/Walk/Sit
SUBJECT 01	35	DAE	15.40	1.13	N/A	4.3	45/30/30
	20	DAE	0.61	0.25	N/A	4.3	30/30/30
	30	DAE	6.18	0.49	N/A	4.3	30/30/30
	30	SoC	1.29	0.53	N/A	4.3	30/30/30
	35	SoC	4.38	0.89	N/A	4.3	30/30/30
	20	SoC	0.06	0.20	N/A	4.3	30/30/30
SUBJECT 02	35	DAE	9.64	0.51	N/A	5.9	30/30/30
	20	DAE	2.53	2.12	N/A	5.9	30/30/30
	30	DAE	4.65	0.51	N/A	5.9	30/30/30
	20	SoC	0.09	0.28	N/A	5.9	30/30/30
	35	SoC	1.47	0.77	N/A	5.9	30/30/30
	30	SoC	1.62	1.46	N/A	5.9	30/31/30

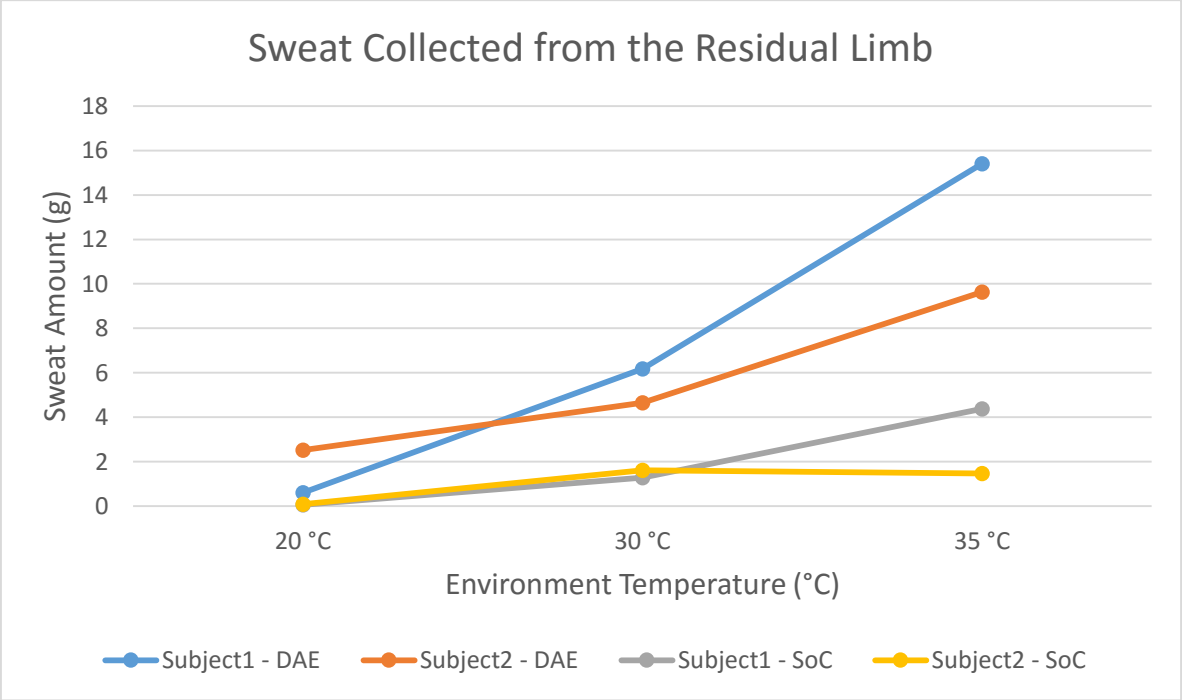

FIGURE 9: SWEAT CAPTURED FROM THE RESIDUAL LIMB DURING EACH TEST.

DISCUSSION

COMPUTATIONAL THERMAL MODEL

The model results show clearly that total cooling power increases with flow velocity for all cases, but a key assumption is that the skin surface is completely and uniformly coated with sweat. A faster flow allows for increased transport rates of energy and water vapor, thereby creating a larger temperature gradient between the skin and air flow. This increases convective cooling which relies on flow velocity and temperature differential. Because evaporation requires a moisture concentration gradient to operate, no evaporative cooling is seen without the presence of some moisture on the skin. The model assumes all skin surface area to be wetted when, in reality, this is not always the case.

The model geometry is based on a simplified shape. The shape of a human leg is more difficult to model mathematically than a simple geometric shape. For this reason, this model assumes a cylindrical leg with the same length and surface area as the thermal manikin for ease of results comparison. Values of the Nusselt number are well documented for flow over a cylinder and not for a human leg. Despite the simplification, values for Nusselt number are still limited by the assumption that the outer surface is adiabatic.

Sweat rate is determined by several external factors including ambient temperature, body insulation, and radiation, as well as internal factors like blood flow, metabolic rate, and work load. The maximum sweat rate calculated for model test conditions (20 °C ambient air at 10% RH) was 1.06×10^{-5} kg/s. For comparison, one study reported a maximum, subject-averaged sweat rate of approximately 5.9 g/min while walking at a pace of 3.3 km/h outside during the summer for 30 minutes [36]. Assume a uniform sweat rate across the entire body and that a single intact leg accounts for roughly 18% of body surface area (based on the “Rule of Nine’s” for burn patient assessment). Assume also that skin surface area covered by a prosthesis for an average transtibial amputee’s residual limb accounts for 1/3 of the whole leg, or approximately 6% of total body surface area. This yields a localized limb sweat rate of approximately 0.59×10^{-5} kg/s. The computational model is currently over estimating the amount of sweat available for evaporative cooling by nearly a factor of two. Actual cooling power may be less than predicted by the model.

The model demonstrates that a DAE system could theoretically lower the skin temperature sufficiently to decrease or even stop sweating at higher flow rates. However, 0.5 m/s air flow against the skin might cause discomfort for the amputee. It should also be noted that this model becomes unstable as the air temperature nears the body’s core temperature. Cause for the instability is likely due to failure of the assumption that flow is laminar at higher velocities.

An alternative model could use a constant heat flux to calculate skin temperature instead of assuming a constant core temperature. Further, the assumption that the liner and socket are

adiabatic insulators could be reconsidered. For the no flow case, the model predicts a skin temperature equal to body core temperature, no matter the ambient conditions. However, in reality, a higher ambient temperature would result in skin temperatures that might exceed body core temperature.

A maximum cooling rate (for tested conditions) of 3 W was achieved at 20 °C ambient air and 10% RH with a flow rate of 0.03 m/s (approximate average flow rate created by the DAE socket). Walking, for non-amputees, is generally considered to be between 1.8 to 5.3 metabolic equivalent tasks (MET's) [37] which translates to between 32 and 93 W. The DAE socket theoretically dissipates 9.4 and 3.2% of the total heat generated by the body during a walking activity, respectively. This could create a stable cooling environment inside the socket. For more metabolically expensive tasks, a DAE socket (for room temperature and low humidity) would at least slow the rise in core temperature and decrease sweating levels for a given period of time.

Because evaporative cooling far outweighs convective cooling, heat removal seems like it should be near zero for air at 100% RH and temperatures lower than body core temperature like they are at body temperature. However, because the vapor saturation limit (i.e., specific humidity) increases with temperature, it is not. For a fixed mass of vapor, relative humidity decreases when temperature increases. For inlet air at 100% relative humidity and body temperature, no evaporative cooling will occur. However, in most cases there will be a positive temperature gradient (i.e., $T_{outlet} > T_{inlet}$). Because specific humidity increases with temperature, air can enter the prosthesis at 100% RH and still allow for some evaporation due to a temperature induced increase in the vapor saturation limit.

At lower relative humidities, ambient air temperature has little effect on heat removal, whereas ambient temperature greatly effects heat removal at higher relative humidities. This is likely because the vapor saturation limit (g/kg) increases exponentially with temperature. For a nearly fixed outlet temperature, the percent difference in mass of evaporated liquid (and consequently cooling potential) for a large air flow temperature gradient is much smaller than at a small temperature gradient.

THERMAL MANIKIN

Despite most of the thermistor wires being embedded in a silicone band under the proximal lip of the liner, a secondary seal of electrical tape over the proximal liner lip, and zip-ties around the limb to compress the liner to the silicone seal, small amounts air may have leaked in through channels created by four thermistor wires that were routed between the silicone seal and the copper. This non-uniform air flow may have produced localized temperature decreases of a larger magnitude than would be experienced over the entire limb.

Another limitation of the thermal manikin is its copper skin. Because copper has high thermal conductivity it transfers heat from the water at body core temperature to the outer skin surface with little resistance (i.e., little change in temperature). The skin surface temperature is essentially equal to body core temperature and has a much higher thermal capacitance than human skin.

Some researchers have stated that a thermal manikin does not respond to its environment as a human body does because its core and skin temperature are constant. In contrast, the human body varies local skin temperature to control the physiological response [20]. This imposes some limitations on the accuracy of results when directly comparing how an amputee's limb will respond to the DAE socket. However, the manikin remains a good indicator of the socket's ability to remove heat from the leg, regardless of physiological responses.

Heat removal from the manikin limb under active DAE cooling is approximately three times greater than predicted by computational model results (21.8 W compared to ~7 W respectively). These values are excessively high and demonstrate that heat energy is escaping the thermal manikin through other means that just DAE. Passive cooling also shows greater energy removal than expected. Many potential causes exist. The manikin may allow more conductive cooling between the skin and ambient air than initially thought or the square foam cover may not have sealed well. HVAC in the room may have also increased heat removal through convection. The bubbler used for mixing the water is pumping in room temperature air. The small band of exposed copper above the proximal lip of the liner (visible in Figure 1) may have acted as a heat sink due to copper's high thermal conductivity. It seems most likely a combination of the last two options were to blame for the majority of heat loss error.

Cooling power results from the manikin may be optimistic. It was designed to match an average lower limb amputee's residual limb. However, if the manikin is larger than the average transtibial amputee's limb, the added surface area would overestimate the cooling advantage.

Power input through the PID controller to the manikin's heater is used to estimate heat removed from the system. However, the current meter used to record heater current has a maximum sample rate of 1 Hz. Once the manikin temperature settles to the set temperature, short heating pulses are sufficient to maintain it. The combination of short current pulses and slow sampling rate leads to an incomplete picture of true power consumption. The general trend was captured in the data, but this is likely the largest source of error.

Two of the 12 skin temperature readings dropped approximately 0.6 °C. One of them was directly under a proximal port while the other was midway down the limb. It is likely that these two thermistors' wires created paths of least resistance for airflow through the sock layer. It follows

that those thermistors experienced increased localized cooling as compared to the other thermistors.

It is not surprising that neither of the passive cooling conditions yielded much change in surface temperatures. The liner and socket are already known to create an insulative environment the greatly hinders conductive cooling. Without additional cooling mechanisms, very little heat can be exchanged to the surroundings.

HUMAN SUBJECTS

Sweat was noticed wicking out of the proximal lip of the liner during the standard of care tests. This was especially true during the post-treadmill rest phase. The proximal liner edge usually slipped distally during walking, exposing skin that had been initially covered. This moisture was either lost to evaporation during walking or was absorbed by a cloth on the chair during the following rest period.

At the time of writing, two subjects have been screened, consented, and successfully completed the full test sequence. Initial data (Table 3) suggests the DAE system may provide increased adherence performance during light activity in extreme heat and humidity. However, neither subject experienced complete loss of adherence. It may be that longer walking durations or more rigorous sessions are needed to better observe and more clearly understand the effects of DAE on limb adherence.

External complications lead to an increased initial acclimation rest time for Subject 01. It is possible that this accounts, in part, for the large discrepancy in sweat levels between the two subjects' 35 °C DAE tests. For Subject 02, a decrease of 0.15 g measured perspiration occurred between the 30 °C test and the 35 °C test. This is does not fit the overall trend that sweat collected increases with environment temperature, regardless of socket type. The subject did experience extreme sagging of the proximal liner lip (> 6 cm). Moisture on the exposed skin surface was almost entirely lost to evaporation and likely is the cause of the discrepancy. Despite the extreme liner migration, the subject was able to complete the walking session without total loss of adherence confidence. It may also be possible that a longer walking period is needed to fully observe the effects of sweat accumulation on limb adherence.

Perspiration levels are higher for when subjects wear the DAE socket as compared to the SoC socket at the same temperature. The DAE's thin sock layer between the skin and the liner could be increasing wicking of sweat away from the skin. Although more moisture initially appears to be an issue, the majority is held either in the manifold below the socket or in the sock (Appendix A). It seems possible that the DAE's active moisture removal could also lead to improved skin conditions when compared to the SoC over extended periods of use. It also seems reasonable

that continued airflow through the DAE socket would dry the limb more rapidly after bouts of increased perspiration than with a SoC socket.

All wetted items were sealed in containers as quickly as possible, but there were undoubtedly some minimal losses due to evaporation. It should also be noted that, despite the manifold's trap design, moisture was found to escape through the exhaust tubing in small quantities. Therefore, collected moisture from both socket systems should be considered conservative measures.

CONCLUSIONS

The computational model demonstrated that heat removal from the limb increases with increasing flow velocity, decreasing ambient air temperature, and decreasing relative humidity. Most notably, as ambient air temperatures near body temperature, relative humidity increasingly becomes the dominant determining factor in heat removal efficiency. The ability to condition the air, specifically lowering the relative humidity of entering air, would be of greatest benefit to the DAE design.

When comparing computational model results to thermal manikin results, skin temperature predictions and measurements were fairly similar. The model predicted an approximate 0.25 °C drop in skin temperature for room temperature (20 °C) ambient air, 30% RH, and a flow velocity of 0.035 m/s. Manikin skin temperatures dropped between 0.2 and 0.6 °C for the similar conditions. Power removed from the limb was inconsistent between the manikin and model though. This was due to several possible avenues for "heat leakage" from the manikin that would not be present in a human limb.

Human subject testing demonstrated that a DAE socket may increase secure adherence ambulation times as compared to a SoC socket. Although little to no sensible limb cooling was observed during the tests, the active moisture removal and slight vacuum suspension may prove useful for amputees requiring secure adherence in sweat intensive environments.

FUTURE WORK

COMPUTATIONAL THERMAL MODEL

The DAE socket is a very complex physical system. This computational model does not account for how airflow reacts to the weave of the sock or the dynamically changing flow channels created by ambulatory loading cycles and pooling moisture. Further work should aim to better understand how these conditions effect heat removal and see if any improvements can be made in cooling efficiency.

It could also be helpful to construct a 3D CAD model of a limb and DAE socket for use in CFD (Computational Fluid Dynamics) analysis. Airflow characteristics through the sock for different

velocities and weave patterns could lead to new insights in material design that would allow perspiration and air to move through the sock more efficiently. Dynamic loading flow characteristics would also interesting to explore.

Another idea for improvement involves estimating the effects of airflow velocity and ambient air temperatures on the relative humidity of the outflow. Currently, the model assumes 100% RH for exiting air under any conditions. This likely does not hold true as flow increases.

THERMAL MANIKIN

Further validation of the accuracy of manikin results could be achieved by testing inside the thermal conditioning chamber used for human subject testing. Results for non-room-temperature tests could be insightful in building a second generation thermal manikin or for making improvements to the existing one. With some modifications to correct for the above listed limitations it also seems testing the efficacy of a PCM containing liner over longer periods of time would prove useful. The most recent tests involved a 25 minute exercise period followed by 10 minutes of rest. Although the technology could prove useful for short bouts of increased activity, it is possible the PCM did not fully melt during this time. The manikin could be used to identify how long it takes for all PCM to melt for a given condition and how cooling is altered after that point.

HUMAN SUBJECTS

Recruiting, enrolling, and testing more human subject will enable statistical testing of the five hypotheses proposed. These additional subjects are key to generalizing the study results from a small sample population.

REFERENCES

[1] K. Ghoseiri, M.R. Safari, Prevalence of heat and perspiration discomfort inside prostheses: Literature review, J. Rehabil. Res. Dev. 51 (2014) 855–868. doi:10.1682/JRRD.2013.06.0133.

[2] K. Hagberg, R. Brånemark, Consequences of non-vascular trans-femoral amputation: a survey of quality of life, prosthetic use and problems., Prosthet. Orthot. Int. 25 (2001) 186–194. doi:10.1080/03093640108726601.

[3] G.K. Klute, G.I. Rowe, a V Mamishev, W.R. Ledoux, The thermal conductivity of prosthetic sockets and liners., Prosthet. Orthot. Int. 31 (2007) 292–299. doi:10.1080/03093640601042554.

[4] P.F.D. Naylor, Experimental Friction Blisters, Br. J. Dermatol. 67 (1955) 327–342. doi:10.1111/j.1365-2133.1955.tb12657.x.

[5] M.B. Sulzberger, T.A. Cortese, L. Fishman, H.S. Wiley, Studies on blisters produced by friction, J. Invest. Dermatol. 47 (1966) 456–465. doi:10.1038/jid.1966.76.

[6] L.-C. Gerhardt, V. Strässle, a Lenz, N.D. Spencer, S. Derler, Influence of epidermal hydration on the friction of human skin against textiles., J. R. Soc. Interface. 5 (2008) 1317–1328. doi:10.1098/rsif.2008.0034.

[7] U. Kern, M. Kohl, U. Seifert, T. Schlereth, Botulinum toxin type B in the treatment of residual limb hyperhidrosis for lower limb amputees: a pilot study., Am. J. Phys. Med. Rehabil. / Assoc. Acad. Physiatr. 90 (2011) 321–329. doi:10.1097/PHM.0b013e31820636fd.

[8] G.K. Klute, E. Huff, W.R. Ledoux, Does Activity Affect Residual Limb Skin Temperatures?, Clin. Orthop. Relat. Res. 472 (2014) 3062–3067. doi:10.1007/s11999-014-3741-4.

[9] J.T. Peery, W.R. Ledoux, G.K. Klute, Residual-limb skin temperature in transtibial sockets., J. Rehabil. Res. Dev. 42 (2005) 147–154. doi:10.1682/JRRD.2004.01.0013.

[10] M. Shibasaki, T.E. Wilson, C.G. Crandall, Neural control and mechanisms of eccrine sweating during heat stress and exercise., J. Appl. Physiol. 100 (2006) 1692–1701. doi:10.1152/japplphysiol.01124.2005.

[11] G.K. Klute, C.F. Kallfelz, J.M. Czerniecki, Mechanical properties of prosthetic limbs: adapting to the patient., J. Rehabil. Res. Dev. 38 (2001) 299–307.

[12] Alpha SmartTemp Liner featuring Outlast, Ohio Willow Wood Co. (n.d.). http://www.willowwoodco.com/products-and-services/liners/transtibial/alpha-smarttemp-liner.

[13] T. Jacobs, S.M. Schneider, S.M.C. Lee, A. McDaniel, Performance of the Liquid-Cooling Garment With the Advanced Crew Escape Suit in Elevated Cabin Temperatures, Houston, TX, 2004.

[14] J. Rugh, C. King, H. Paul, L. Trevino, G. Bue, Phase II Testing of Liquid Cooling Garments

Using a Sweating Manikin , Controlled by a Human Physiological Model, Engineering. (2006). doi:10.4271/2006-01-2239.

[15] A. Kurbak, O. Kayacan, Effect of Garment Design on Liquid Cooling Garments, Text. Res. J. 80 (2010) 1442–1455. doi:10.1177/0040517509358800.

[16] Y. Han, F. Liu, G. Dowd, J. Zhe, A thermal management device for a lower-limb prosthesis, Appl. Therm. Eng. 82 (2015) 246–252. doi:10.1016/j.applthermaleng.2015.02.078.

[17] C.M. Webber, B.L. Davis, Design of a novel prosthetic socket : Assessment of the thermal performance, J. Biomech. 48 (2015) 1294–1299. doi:10.1016/j.jbiomech.2015.02.048.

[18] M.M. Wernke, R.M. Schroeder, C.T. Kelley, J.A. Denune, J.M. Colvin, SmartTemp Prosthetic Liner Significantly Reduces Residual Limb Temperature and Perspiration, JPO J. Prosthetics Orthot. 27 (2015) 134–139.

[19] X. Xu, J. Werner, A Dynamic Model of the Human/Clothing/Environment-System, Appl. Hum. Sci. 16 (1997) 61–75.

[20] R. McGuffin, R. Burke, Z. Hui, Charley Huizenga, A. Vlahinos, G. Fu, Human Thermal Comfort Model and Manikin, SAE Pap. 2002-01-1955. (2002). doi:10.4271/2002-01-1955.

[21] Y. Cengel, M. Boles, Thermodynamics: An Engineering Approach, 6th Editio, McGraw-Hill Education, New York, NY, 2006. https://books.google.com/books?id=q2SiPgAACAAJ.

[22] O. Akkus, A. Oguz, M. Uzunlulu, M. Kizilgul, Evaluation of Skin and Subcutaneous Adipose Tissue Thickness for Optimal Insulin Injection, J. Diabetes Metab. 03 (2012) 216–220. doi:10.4172/2155-6156.1000216.

[23] J.T. Peery, G.K. Klute, J.J. Blevins, W.R. Ledoux, A three-dimensional finite element model of the transibial residual limb and prosthetic socket to predict skin temperatures., IEEE Trans. Neural Syst. Rehabil. Eng. 14 (2006) 336–43. doi:10.1109/TNSRE.2006.881532.

[24] T.L. Bergman, A.S. Lavine, F.P. Incropera, Fundamentals of Heat and Mass Transfer, 7th Edition, 7th Editio, John Wiley & Sons, Incorporated, Jefferson City, 2011. https://books.google.com/books?id=5cgbAAAAQBAJ.

[25] L.H. Aulick, S. Robinson, S.P. Tzankoff, Arm and leg intravascular temperatures of men during submaximal exercise, J. Appl. Physiol. 51 (1981) 1092–1097. http://jap.physiology.org/content/51/5/1092.abstract.

[26] T. Clarke Jr., Chauncy, the Copper Thermal Manikin, Mil. Med. 180 (2015) 718–719. doi:10.7205/MILMED-D-15-00004.

[27] T.L. Madsen, A new generation of thermal manikins, Therm. Insul. Lab. Tech. Univ. Denmark. (1989).

[28] R. Burke, J. Rugh, R. Farrington, ADAM--the Advanced Automotive Manikin, in: 5th Int. Meet. Therm. Manikins Model. Strasbourg, Fr., 2003.

[29] J. Lustbader, Evaluation of advanced automotive seats to improve thermal comfort and fuel economy, in: 7th Veh. Therm. Manag. Syst. Conf. Exhib., Society of Automotive

Engineers, Toronto, Canada, n.d. doi:10.4271/2005-01-2056.

[30] I. Holmér, Thermal manikin history and applications., Eur. J. Appl. Physiol. 92 (2004) 614–8. doi:10.1007/s00421-004-1135-0.

[31] K. Bates, G. Klute, Thermal Residual Limb Manikin to Test Novel Cooling Technologies for Prosthetic Sockets, in: ASME 2013 Summer …, Sunriver, OR, 2013: pp. 1–2. http://proceedings.asmedigitalcollection.asme.org/ (accessed October 9, 2014).

[32] ASTM Standard F1291-10, Standard Test Method for Measuring the Thermal Insulation of Clothing Using a Heated Manikin, (2010) 1990. www.astm.org.

[33] ASTM Standard F2370-10, Standard Test Method for Measuring the Evaporative Resistance of Clothing Using a Sweating Manikin, ASTM Int. (2005) 2010.

[34] ASTM Standard F1868-14, Standard Test Method for Thermal and Evaporative Resistance of Clothing Materials Using a Sweating Hot Plate, West Conshohocken, PA, 1998.

[35] ASTM Standard F2371-10e1, Standard Test Method for Measuring the Heat Removal Rate of Personal Cooling Systems Using a Sweating Heated Manikin, West Conshohocken, PA, 2005.

[36] A. Yoshida, S. Taketani, Experimental Analysis of Human Thermal Condition During Outdoor Exercise under Summer Conditions, J. Heat Isl. Inst. Int. 9 (2014) 33–38.

[37] M. Jetté, K. Sidney, G. Blümchen, Metabolic equivalents (METS) in exercise testing, exercise prescription, and evaluation of functional capacity., Clin. Cardiol. 13 (1990) 555–565. doi:10.1002/clc.4960130809.

ACKNOWLEDGEMENTS

The author gratefully acknowledges the support of the U.S. Department of the Army and the U.S. Department of Veterans Affairs for the following grant support:

1. Dept. of the Army, Advanced Prosthetics and Human Performance, US Army Medical Research & Materiel Command at the Telemedicine and Advanced Technology Research Center, grant W81XWH-11-2-0169

2. Dept. of Veterans Affairs, Rehabilitation Research and Development Service, grant IO1 RX000901C

In addition, the author would like to thank, Glenn Klute, for his instrumental role in guiding and advising the research, Jocelyn Berge for her key role in human subjects testing, Charles King for his collaboration on the DAE socket, and Jan Pecararo for subject recruitment.

APPENDIX A

Grams of Sweat for Varying Conditions	COPA 01						COPA 02					
	DAE			SoC			DAE			SoC		
	20°C	30°C	35°C	20°C	30°C	35°C	20°C	30°C	35°C	20°C	30°C	35°C
Humidity Tee	0.05	0.04	0.05	-	-	-	0.07	0.02	0.28	-	-	-
Pump Tubing	0.09	0.05	0.04	-	-	-	0.01	0.03	0.02	-	-	-
Manifold	0.44	0.40	3.35	-	-	-	0.41	0.33	0.58	-	-	-
Limb & Liner Wipes	0.03	0.10	0.44	0.02	1.22	4.34	0.03	0.00	0.01	0.06	1.59	1.48
Sock	0.06	5.45	11.35	-	-	-	2.00	4.22	8.66	-	-	-
Sweat Patch	0.25	0.49	1.13	0.20	0.53	0.89	2.12	0.51	0.51	0.28	1.46	0.77
Gloves	0.12	0.14	0.17	0.04	0.07	0.04	0.07	0.05	0.09	0.03	0.03	0.01
Q-tips	-	-	-	-	-	-	0.04	0.04	0.03	-	-	-
Total w/o Sweat Patch	0.61	6.18	15.40	0.06	1.29	4.38	2.53	4.65	9.64	0.09	1.62	1.47
Liner Slip (mm)	NR	NR	NR	7	20	18	41	33	63	8	30	70
Water Consumed (fl. Oz.)	2	NR	NR	8	14	12	-	-	24	1	28	32

NR – Not Recorded